

# A New Concept Linking Observable Stable Isotope Fractionation to Transformation Pathways of Organic Pollutants

MARTIN ELSNER,\*<sup>†</sup> LUC ZWANK,<sup>†,‡</sup> DANIEL HUNKELER,<sup>§</sup> AND RENE P. SCHWARZENBACH<sup>†</sup>

Swiss Federal Institute for Environmental Science and Technology (EAWAG)

Swiss Federal Institute of Technology Zurich (ETHZ), Ueberlandstrasse 133, CH-8600 Duebendorf

Switzerland, and Centre of Hydrogeology, University of Neuchâtel, Rue Emile Argand 11, CH-2007 Neuchâtel, Switzerland

Measuring stable isotope fractionation of carbon, hydrogen, and other elements by Compound Specific Isotope Analysis (CSIA) is a new, innovative approach to assess organic pollutant degradation in the environment. Central to this concept is the Rayleigh equation which relates degradation-induced decreases in concentrations directly to concomitant changes in bulk (= average over the whole compound) isotope ratios. The extent of in situ transformation may therefore be inferred from measured isotope ratios in field samples, provided that an appropriate enrichment factor ( $\epsilon_{\text{bulk}}$ ) is known. This  $\epsilon_{\text{bulk}}$  value, however, is usually only valid for a specific compound and for specific degradation conditions. Therefore, a direct comparison of  $\epsilon_{\text{bulk}}$  values for different compounds and for different types of reactions has in general not been feasible. In addition, it is often uncertain how robust and reproducible  $\epsilon_{\text{bulk}}$  values are and how confidently they can be used to quantify contaminant degradation in the field. To improve this situation and to achieve a more in-depth understanding, this critical review aims to relate fundamental insight about kinetic isotope effects (KIE) found in the physico(bio)chemical literature to apparent kinetic isotope effects (AKIE) derived from  $\epsilon_{\text{bulk}}$  values reported in environmentally oriented studies. Starting from basic rate laws, a quite general derivation of the Rayleigh equation is given, resulting in a novel set of simple equations that take into account the effects of (1) nonreacting positions and (2) intramolecular competition and that lead to position-specific AKIE values rather than bulk enrichment factors. Reevaluation of existing  $\epsilon_{\text{bulk}}$  literature values result in consistent ranges of AKIE values that generally are in good agreement with previously published data in the (bio)-chemical literature and are typical of certain degradation reactions (subscripts C and H indicate values for carbon and hydrogen):  $\text{AKIE}_{\text{C}} = 1.01\text{--}1.03$  and  $\text{AKIE}_{\text{H}} = 2\text{--}23$  for oxidation of C–H bonds;  $\text{AKIE}_{\text{C}} = 1.03\text{--}1.07$  for  $\text{S}_{\text{N}}2$ -

reactions;  $\text{AKIE}_{\text{C}} = 1.02\text{--}1.03$  for reductive cleavage of C–Cl bonds;  $\text{AKIE}_{\text{C}} = 1.00\text{--}1.01$  for C=C bond epoxidation;  $\text{AKIE}_{\text{C}} = 1.02\text{--}1.03$  for C=C bond oxidation by permanganate. Hence, the evaluation scheme presented bridges a gap between basic and environmental (bio)chemistry and provides insight into factors that control the magnitude of bulk isotope fractionation factors. It also serves as a basis to identify degradation pathways using isotope data. It is shown how such an analysis may be even possible in complex field situations and/or in cases where AKIE values are smaller than intrinsic KIE values, provided that isotope fractionation is measured for two elements simultaneously (“two-dimensional isotope analysis”). Finally, the procedure is used (1) to point out the possibility of estimating approximate  $\epsilon_{\text{bulk}}$  values for new compounds and (2) to discuss the moderate, but non-negligible variability that may quite generally be associated with  $\epsilon_{\text{bulk}}$  values. Future research is suggested to better understand and take into account the various factors that may cause such variability.

## Introduction

In recent years Compound Specific Isotope Analysis (CSIA) has undergone a rapid development toward important new applications in contaminant hydrology and organic (bio)-geochemistry. With CSIA, the relative abundance of the heavy ( $^{\text{h}}\text{E}$ ) and light ( $^{\text{l}}\text{E}$ ) isotopes of a given element E is determined in molecules of a given compound, expressed by the ratio  $R = ^{\text{h}}\text{E}/^{\text{l}}\text{E}$ . Such bulk isotope ratios (= ratios averaged over the bulk compound) can be measured by gas chromatography–isotope ratio mass spectrometry (GC–IRMS) and are reported as difference in per mil  $\delta^{\text{h}}\text{E}$  with respect to an international reference standard (1, 2):

$$\delta^{\text{h}}\text{E} = \left( \frac{R - R_{\text{ref}}}{R_{\text{ref}}} \right) \cdot 1000\text{‰} = \left( \frac{(^{\text{h}}\text{E}/^{\text{l}}\text{E}) - (^{\text{h}}\text{E}/^{\text{l}}\text{E})_{\text{ref}}}{(^{\text{h}}\text{E}/^{\text{l}}\text{E})_{\text{ref}}} \right) \cdot 1000\text{‰} \quad (1)$$

Presently, online GC–IRMS analysis is possible for the elements hydrogen ( $^2\text{H}/^1\text{H}$ ), carbon ( $^{13}\text{C}/^{12}\text{C}$ ), nitrogen ( $^{15}\text{N}/^{14}\text{N}$ ), and oxygen ( $^{18}\text{O}/^{16}\text{O}$ ). A short discussion of experimental details is given in the Supporting Information. More information is provided by comprehensive reviews of Brenna (3) and Meier-Augenstein (4) as well as in papers on the original method development by Hayes and co-workers (5–7). The online coupling of IRMS to chromatographic separa-

\* Corresponding author phone: ++1 416 978 0825; fax: ++1 416 978 3938; e-mail: martin.elsner@utoronto.ca. Present address: Stable Isotope Laboratory, Department of Geology, University of Toronto, 22 Russell Street, Toronto, Ontario M5S 3B1, Canada.

<sup>†</sup> EAWAG and ETHZ.

<sup>§</sup> University of Neuchâtel.

<sup>‡</sup> Present address: Centre de Recherche Public Henri Tudor, Centre de Ressources des Technologies de l'Environnement (CRTE), Technoport Schlassgoart, 66, rue de Luxembourg, B.P. 144, L-4002 Esch-sur-Alzette, Luxembourg.

tion methods has made it possible to analyze bulk isotope ratios of organic compounds in small, environmentally relevant concentrations. In the case of carbon isotopes, method quantification limits have been achieved in the low ppm (mg/L) range with liquid–liquid extraction (8) and headspace analysis (9, 10), while enrichment methods such as solid-phase microextraction and purge and trap have lowered the limits even further to the low ppb ( $\mu\text{g/L}$ ) range (10–12). As studies in contaminant hydrology have so far primarily focused on measurements of  $\delta^2\text{H}$  and, particularly,  $\delta^{13}\text{C}$ , this review will mostly deal with these two elements.

The way in which CSIA is currently used to assess groundwater contaminations was pioneered in studies by Sherwood-Lollar et al. (13), Heraty et al. (14), Meckenstock et al. (15), and Hunkeler et al. (16, 17). A common fundamental assumption of these first publications is that the bulk isotope fractionation associated with degradation of organic pollutants appears to follow the Rayleigh equation. This classical relationship was originally derived for fractionation in the diffusion of gases (18) and was later also used to describe kinetic isotope fractionation in geology (1, 2, 19), marine sciences (20), chemistry (21, 22), and biochemistry (23). This equation is extremely useful, because it relates differences in bulk isotope ratios  $\Delta\delta^{\text{hE}}$  directly to changes in contaminant concentrations. Isotope ratios may therefore be used to quantify *how much* degradation has occurred in natural systems. This is especially important if contaminant concentrations decrease not only due to degradation but also due to dilution, sorption, and other processes that are not or only little fractionating. The concept has been confirmed in a number of studies, and comprehensive recent reviews about the use of CSIA to quantify contaminant degradation in the field have been published by Schmidt et al. (12) and Meckenstock et al. (24).

However, despite its great usefulness, several aspects remain unsatisfactory with respect to the way in which the Rayleigh equation is currently applied.

Although the relationship can be derived mathematically for “simple” molecules (only one isotopic atom per element of interest) and one-step, first-order reactions, it is presently not well understood if the equation is generally applicable for more complex situations. By using the Rayleigh equation as a descriptive empirical relationship rather than a well understood physicochemical law, one misses the opportunity to gain important mechanistic information that is inherently present in the observable isotope fractionation. Specifically, it is often uncertain what controls the magnitude of bulk isotope fractionation and how confidently changes in measured bulk isotope ratios can be used to quantify pollutant degradation in the field. Moreover, it is difficult to compare bulk isotope fractionation in different compounds. Finally, one cannot easily discern characteristic patterns for different types of reactions, despite the fact that such information is already published in the form of position-specific kinetic isotope effects in the classical (bio)chemical literature.

The main goal of this critical review is to present and discuss a procedure that makes it possible to derive position-specific apparent kinetic isotope effects (AKIEs) from observed isotope fractionation data of organic pollutant transformation. It is shown how the comparison of the obtained AKIEs with known KIEs can help to identify degradation pathways and provide insight into factors controlling the fundamental variability of observable isotope fractionation. The first part of this article reviews the factors that control the magnitude of kinetic isotope effects (KIEs) in elementary chemical reactions and summarizes published reference values for typical transformation reactions. A general derivation of the Rayleigh equation is then performed starting from simple rate laws and resulting in a novel set of simple

equations that allow calculating AKIE values from observable isotope fractionation data. A rigorous mathematical treatment is given in the Supporting Information, while the main features are explained in the text. Subsequently, existing  $\epsilon_{\text{bulk}}$  literature values are reevaluated, and AKIE values are discussed for different well characterized transformation reactions. With the proposed evaluation procedure and its application to a broad range of major groundwater contaminants, the paper aims to bridge a current gap between contaminant hydrology and the classical (bio)chemical literature.

## Origin and Magnitude of Isotope Fractionation: Kinetic Isotope Effects

Although in complex environmental systems, the magnitude of isotope fractionation occurring during transport and transformation of a given pollutant can depend on many factors, a few important general rules may nevertheless be drawn from the chemical and biochemical literature (21–23, 25, 26). When considering organic contaminants in groundwater, usually, several atoms of a given element E (e.g., E = H, C, N, O, S, Cl) are present at various locations within a larger organic molecule. For this element, significant isotope fractionation can then only be expected at those positions, where covalent bonds involving the element E directly or indirectly (= adjacent to the reactive center) are broken or formed during the rate-limiting step(s) of a given process. Processes that act on the compound as a whole such as advective–dispersive transport, volatilization (9, 10, 27–31), sorption/desorption (29, 32, 33) or binding to an enzyme (33, 34) cause much smaller changes in the overall isotope composition, which are often not detectable within the precision of the analytical method (9, 29, 32).

When considering a reaction in which a specific bond is broken, the elements involved in the reaction will generally show a *normal* isotope effect, that is, the molecules with the heavier isotope at this specific location will react more slowly than those exhibiting a lighter isotope. Using (pseudo)-first-order rate constants  ${}^{\text{l}}k$  and  ${}^{\text{h}}k$ , that quantify the specific reaction rates of the lighter and heavier atom of the element E, an intrinsic kinetic isotope effect  $\text{KIE}_{\text{E}}$ , can be defined as

$$\text{KIE}_{\text{E}} = \frac{{}^{\text{l}}k}{{}^{\text{h}}k} \quad (2)$$

In this review we will consider primarily reactions exhibiting *normal* isotope effects ( $\text{KIE}_{\text{E}} > 1$ ), although *inverse* isotope effects ( $\text{KIE}_{\text{E}} < 1$ ) may be observed in cases in which bonds are strengthened or formed in the rate-limiting step(s) (35–37). Isotope effects are called *primary*, if the element E is directly present in the reacting bond, whereas they are *secondary*, if E is located adjacent to the reacting position. The direct experimental measurement of kinetic isotope effects is generally accomplished with isotopically labeled substrates (38, 39). Since very recently, also substrates of natural isotopic abundance are used provided that substances can be brought to partial reaction, recovered completely, and can subsequently be analyzed for position-specific isotope changes using SNIF-NMR (Site-Specific Natural Isotope Fractionation by Nuclear Magnetic Resonance Spectroscopy) (40, 41).

**Some “Rules of Thumb” for Qualitative Predictions of Isotope Effects.** Isotope effects arise only from those changes in molecular energy that are mass-sensitive, in particular from changes in vibrational energies (caused by vibrations of atoms inside a molecule). They do not depend on electronic energies, which are by far the most important ones in determining the activation energy of a given reaction (42). As a consequence, kinetic isotope effects are generally *not*

**TABLE 1. Streitwieser Semiclassical Limits for Isotope Effects at 25 °C<sup>a</sup>**

bond	frequency (cm <sup>-1</sup> )	isotope	KIE
C–H	2900	<sup>12</sup> C/ <sup>13</sup> C	1.021
C–H	2900	<sup>1</sup> H/ <sup>2</sup> H	6.4
C–C	1000	<sup>12</sup> C/ <sup>13</sup> C	1.049
C–Cl	750	<sup>12</sup> C/ <sup>13</sup> C	1.057
C–Cl	750	<sup>35</sup> Cl/ <sup>37</sup> Cl	1.013
C–N	1150	<sup>12</sup> C/ <sup>13</sup> C	1.060
C–N	1150	<sup>14</sup> N/ <sup>15</sup> N	1.044
C–O	1100	<sup>12</sup> C/ <sup>13</sup> C	1.061
C–O	1100	<sup>16</sup> O/ <sup>18</sup> O	1.067

<sup>a</sup> Modified from ref 35. The calculation takes into account only differences in vibrational energies and assumes that the bond is completely broken in the transition state. Contribution of molecular masses and moments of inertia to the isotope effect are neglected. The limits are denoted as semiclassical because no corrections for tunneling are made.

directly correlated to reaction rates. (Sometimes there may, however, be a simultaneous dependence of both observables on a third parameter such as temperature, geometry of transition state, etc., see below.) Since the vibrational energies of a molecule depend strongly on atomic masses and bond strengths as expressed by the force constant of the vibrating bond (see the detailed discussion in the Supporting Information, part 2), it is these parameters that have the greatest influence on kinetic isotope effects (22). In the framework of the transition state theory and using the so-called “zero-point energy approximation” (35) the following rules of thumb can be derived that may be used to make qualitative predictions about isotope effects (for a detailed derivation see the Supporting Information, part 2).

(1) *Influence of Isotope Masses.* The highest fractionation may be expected for elements E that have the greatest relative mass difference between their heavy and light isotopes <sup>b</sup>E and <sup>l</sup>E. Isotope effects observed for hydrogen, for example (100% mass difference between  $m_H = 1$  and  $m_D = 2$ ), are generally much larger than effects for carbon (only 8% mass difference between  $m_{12C} = 12$  and  $m_{13C} = 13$ ).

(2) *Influence of Bonding Partner(s).* For a given element that is present in covalent bonds of a comparable force constant, isotope effects tend to be greater if the element is bound to heavier atoms. Carbon isotope effects, for example, are generally larger in cleavage of C–O or C–Cl bonds, compared to the cleavage of C–H bonds (see Table 1).

(3) *Influence of Changes in Bond Strength.* Isotope effects are generally larger the more the strength of bonds is changed between the ground state and the transition state during a

given reaction. In the case of primary isotope effects associated with bond cleavage this change is greatest if the bond is completely broken in the transition state. Within a set of very closely related reactions involving atoms of the same elements, isotope effects are therefore greater the larger the initial bond force constant is, and they can be expected to increase with increasing extent of bond breakage in the transition state (35). Note that according to the Hammond Postulate, small changes in bonding are expected in early transition states that have substrate-like character, whereas large changes in bonding are associated with late, product-like transition states (43). Exceptions are reactions where breakage of one bond is accompanied by the simultaneous formation of a new bond (e.g., with transfer of hydrogen in any form (proton/hydride/radical) as well as in S<sub>N</sub>2-reactions). Here, maximum isotope effects for the transferred element (H or C, respectively) are observed in symmetric transition states that involve equal parts of bond cleavage and formation (22, 44).

(4) *Secondary Isotope Effects.* Compared to primary isotope effects, changes in bonding are much smaller in the case of secondary isotope effects, where positions adjacent to the reacting bond are only slightly affected by the proximity to the reaction center, for example through changes in coordination geometry (45). Thus for the same element, secondary isotope effects are generally at least 1 order of magnitude smaller than primary isotope effects (46, 47).

(5) *Stabilization at the Reactive Position by Adjacent Bonds.* Although the same reactive position containing the same element(s) may react in a seemingly similar way, adjacent bonds can play different roles in stabilizing the transition state structure. The net isotope effect at the reacting position is then caused by the contributions of *all* participating bonds. For example, if a C–Cl bond is broken in the hydrolysis of chlorinated alkanes, large carbon isotope effects at the reacting C atom may be expected for a concerted substitution mechanism (S<sub>N</sub>2), but they are much smaller in a dissociation–association mechanism (S<sub>N</sub>1), where loss in bonding is compensated by increased stabilization of all adjacent bonds to the reacting C atom (see Table 2 and section 8.3.4 in ref 22; exemplary schemes of S<sub>N</sub>1 and S<sub>N</sub>2 reactions are given in Scheme 1.)

(6) *Concerted Reactions: Effects in Several Positions.* Although bond changes are often confined to only one reactive bond, in more complicated cases a reaction may be concerted, and isotope effects occur at several locations simultaneously. For example, reductive transformation of chlorinated ethanes and ethenes may involve initial cleavage of only one C–Cl bond or engage both carbon atoms simultaneously (48, 49). Also in the oxidation of double bonds or aromatic compounds, the reaction may either be localized

**TABLE 2. Experimentally Determined Kinetic Isotope Effects for Important Types of Chemical Reactions<sup>a</sup>**

type of reaction	isotope	KIE	ref
reactions involving hydrogen (e.g., H-radical transfer in oxidation reactions)	<sup>12</sup> C/ <sup>13</sup> C	1.015 (1 study)	(47)
	<sup>1</sup> H/ <sup>2</sup> H	generally > 2, typically 3–8, up to 40–50	(52–55)
nucleophilic substitution (S <sub>N</sub> 2 type) involving C–Cl, C–N, C–O bonds etc.	<sup>12</sup> C/ <sup>13</sup> C	1.03–1.09	(56)
	<sup>1</sup> H/ <sup>2</sup> H (secondary)	0.95–1.05 (next to reacting bond)	(22), p 304 in ref 46
nucleophilic substitution (S <sub>N</sub> 1 type) involving C–Cl, C–N, C–O bonds etc.	<sup>12</sup> C/ <sup>13</sup> C	1.00–1.03	(56)
	<sup>1</sup> H/ <sup>2</sup> H (secondary)	1.1–1.2 (next to reacting bond) 1.05–1.15 (one bond apart)	(22, 46)
oxidation of C=C bonds with permanganate (average over both C atoms)	<sup>12</sup> C/ <sup>13</sup> C	1.024 (1 study)	(57, 58)
epoxidation of C=C bonds (average over both C atoms)	<sup>12</sup> C/ <sup>13</sup> C	1.011 (1 study)	(50)

<sup>a</sup> Original reference data are discussed in more detail in the Supporting Information.



to only one carbon atom or involve both adjacent atoms such as during epoxidation (50). If in such a concerted reaction, both centers experience the change in bonding to the same extent, the reaction is said to be synchronous, whereas it is asynchronous if one center is more engaged than the other. Applying labeled substrate or SNIF-NMR (Site-Specific Natural Isotope Fractionation by Nuclear Magnetic Resonance Spectroscopy), it is sometimes possible even in such complicated cases to determine isotope effects in each reacting position and thus to investigate whether a reaction occurs stepwise, asynchronous or synchronous (40). Using substrates of natural isotopic abundance in combination with isotope analysis by GC-IRMS, however, one can only determine an average isotope fractionation, and without previous mechanistic knowledge this fractionation must then be attributed to all potentially reactive positions, whether they are involved in the rate-limiting step or not.

#### Semiquantitative Estimates of Kinetic Isotope Effects.

Based on the rules of thumb (1)–(3) listed above, it is possible to estimate approximate *maximum* kinetic isotope effects (“semiclassical Streitwieser Limits”) for the breakage of typical chemical bonds (35). Such numbers are derived from greatly simplifying assumptions. Only the vibrational energy of the broken bond is considered, and important other factors are neglected: (i) the contributions from additional bonds; (ii) other forms of energy (rotation, translation (35)); (iii) the motion of the transferred atom (described by imaginary vibrational frequencies and known as temperature independent factor (36, 37)); (iv) the effect of hydrogen tunneling (i.e., the ability of hydrogen vs deuterium atoms to cross activation energy barriers by quantum mechanical tunneling (22, 51)). In contrast to more sophisticated approaches that take into account these contributions, Streitwieser Limits can, therefore, have only semiquantitative character (see also discussion in the Supporting Information, part 2). Typical numbers for some important bonds are summarized in Table 1. Note that these values are estimates for complete bond cleavage in an infinitely late transition state. Realistic values with transition states at about 50% bond cleavage would be expected to be half as pronounced, for example  $\text{KIE}_C = 1.01$  (C–H bond) and  $\text{KIE}_C = 1.03$  (C–Cl bond).

**Typical Values of Kinetic Isotope Effects.** For several important types of chemical reactions, kinetic isotope effects have been studied extensively. A summary of typical values is given in Table 2. Comparison with Table 1 shows that the tabulated Streitwieser Limits may indeed be useful to determine an *approximate* magnitude of expected isotope effects. As is demonstrated in Table 2, however, the real values depend not only on the type of chemical bond but also strongly on the type of reaction mechanism. Isotope effects for cleavage of a C–O or C–Cl bond are, for example, small in an  $\text{S}_{\text{N}}1$  reaction and large in an  $\text{S}_{\text{N}}2$  reaction, in accordance with the rules of thumb above. Moreover, actual values may even be larger than the calculated Streitwieser Limit, owing to the motion of the transferred atom and contributions of tunneling, aspects that were not taken into account in the estimate. Finally, Table 2 illustrates that even for the same type of reaction considerable variation may occur, owing to the dependence of isotope effects on the exact structure of the transition state.

**Influence of the Rate-Determining Step/Commitment to Catalysis.** When comparing such KIE data to values that are derived from measurements in more complex systems, it is important to realize that intrinsic isotope effects KIE can only be directly observed if the bond changes involving element E represent the rate-determining step in the overall process. Occasionally, the bond conversion is preceded by a not or only slightly fractionating process such as, for example, transport to reactive sites, adsorption to reactive surfaces, or formation of enzyme–substrate complexes in

biotransformations. If the reverse step of this preceding process is very slow, every substrate molecule that reaches the reactive site will essentially be converted, irrespective of its isotopic composition. Hence, no or only minor isotopic discrimination will be observed in the remaining substrate. The measured *apparent* kinetic isotope effect (AKIE) will then be close to unity, despite the fact that there would be a pronounced *intrinsic* kinetic isotope KIE in the actual bond conversion. One may say that the intrinsic KIE has been masked. This phenomenon has been given different names in different disciplines. In geology the expression “quantitative conversion” is used meaning that the transport/sorption step proceeds quantitatively in the forward direction and the reverse direction of this preceding step is negligible. (Note, however, that for masking it is the *kinetics* of this preceding step that is important, not the net flux.) In biochemistry Northrop introduced the expression “commitment to catalysis” (59). If commitment to catalysis is high, the bond changes involving element E are fast in comparison to the reverse steps of all preceding processes. As discussed above, the intrinsic isotope will then be masked. For the case of labeled substrate Northrop (59) has derived the relationship

$$\text{AKIE}_{\text{labeled substrate}} = \frac{C + \text{KIE}}{C + 1} \quad (3)$$

where “C” is a mathematical expression that can be written in terms of rate constants and is a measure for the commitment to catalysis. (Note that in the biochemical literature, AKIEs are generally denoted as the ratio  $^1(V/K)/^h(V/K)$  where  $V$  are the maximum reaction rates that would be measured with the differently labeled molecules in separate batches, and  $K$  are the respective Michaelis–Menten constants (60)). As is expressed by this formula, in the case of very small commitment to catalysis ( $C \approx 0$ ) the masking is negligible ( $\text{AKIE} \approx \text{KIE}$ ). Although this mathematical concept has been derived for enzyme kinetics, it is important to realize that it may easily be adopted to understand also other reactions of zero- and fractional order involving surface catalysis or transport limitation.

#### Quantification of Isotope Fractionation: Bulk Enrichment and the Rayleigh Equation

To illustrate how changes in isotope signatures of a substrate occurring during a reaction can be quantified in a relatively simple manner, we start out with a reaction in which the observed isotope fractionation can be directly linked to the corresponding KIE value (eq 2). We consider the reductive dehalogenation of carbon tetrachloride ( $\text{CCl}_4$ ) by a reduced iron porphyrin in homogeneous aqueous solution. In this dissociative electron-transfer reaction, a carbon–chlorine bond is broken in the rate-limiting step (61). According to the rule of the geometric mean (see, e.g., discussion in ref 42) the discrimination between  $^{13}\text{C}$  and  $^{12}\text{C}$  is the same in a C– $^{35}\text{Cl}$  as in a C– $^{37}\text{Cl}$  bond and can therefore in both cases be described by the ratio  $^{13}k/^{12}k$ . As is evident from the  $\delta^{13}\text{C}$  values shown in Figure 1a, during the course of the reaction, a continuous significant enrichment of  $^{13}\text{CCl}_4$  molecules in the unreacted pool of  $\text{CCl}_4$  is observed. Since, in this case, there is only one carbon atom present at which the reaction occurs and since the reaction is well-defined, the data can be analyzed using the intrinsic kinetic isotope effect approach

$$\frac{d[^{13}\text{CCl}_4]}{d[^{12}\text{CCl}_4]} = \frac{^{13}k \cdot [^{13}\text{CCl}_4]}{^{12}k \cdot [^{12}\text{CCl}_4]} = \alpha \cdot \frac{[^{13}\text{CCl}_4]}{[^{12}\text{CCl}_4]} \quad (4)$$

where  $\alpha$  is referred to as fractionation factor, which in this case just the reciprocal KIE value, i.e.,  $\alpha = \text{KIE}_C^{-1}$ . Note that in geo- and environmental sciences, in contrast to classical

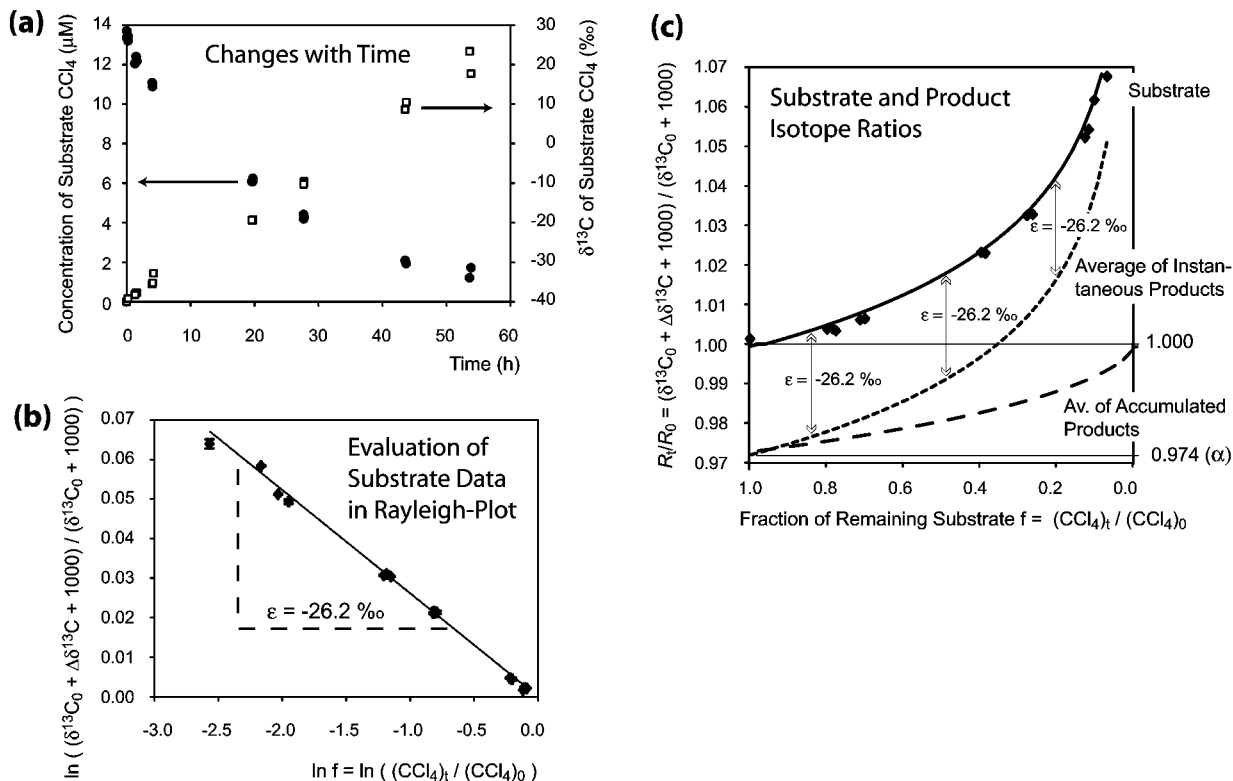


**FIGURE 1. Carbon-isotope fractionation measured during reductive dehalogenation of carbon tetrachloride (CCl<sub>4</sub>) by a reduced iron porphyrin (62). (a) Changes of CCl<sub>4</sub> concentration (solid circles) and isotope ratio (open squares) with time. (b) Rayleigh-Plot (eq 7). (c) Calculated substrate (eq 6) and product ratios using the value of  $\epsilon = -26.2\%$ . (Average product ratios were calculated according to ref 22, chapter 4).**

isotope (bio)chemistry, the ratio of the heavy to light isotope (and not vice versa) is commonly used.

Integration of eq 4 yields (for details see the Supporting Information)

$$\frac{R}{R_0} = \left[ f \cdot \frac{(1 + R_0)}{(1 + R)} \right]^{(\alpha-1)} \quad (5)$$

where  $R$  and  $R_0$  are the <sup>13</sup>C/<sup>12</sup>C ratios in CCl<sub>4</sub> at time  $t$  (no subscript) and time zero (subscript "0"), respectively, and  $f = [\text{CCl}_4]_t / [\text{CCl}_4]_0$  is the remaining fraction of (total) CCl<sub>4</sub> at time  $t$ . Using the  $\delta^{13}\text{C}$  notation (eq 1) and recognizing that, at low natural abundance of the heavier isotope,  $(1+R)/(1+R_0) \approx 1$ , eq 5 can be rewritten and simplified to

$$\frac{R}{R_0} = \frac{(1000 + \delta^{13}\text{C})}{(1000 + \delta^{13}\text{C}_0)} = \frac{(1000 + \delta^{13}\text{C}_0 + \Delta\delta^{13}\text{C})}{(1000 + \delta^{13}\text{C})} \approx f^{(\alpha-1)} = f^{\epsilon/1000} \quad (6)$$

or in logarithmic form

$$\ln \frac{R}{R_0} = \ln \frac{(1000 + \delta^{13}\text{C})}{(1000 + \delta^{13}\text{C}_0)} = \ln \frac{(1000 + \delta^{13}\text{C}_0 + \Delta\delta^{13}\text{C})}{(1000 + \delta^{13}\text{C}_0)} \approx (\alpha - 1) \cdot \ln f = \frac{\epsilon}{1000} \cdot \ln f \quad (7)$$

where  $\Delta\delta^{13}\text{C}$  ( $= \delta^{13}\text{C} - \delta^{13}\text{C}_0$ ) is the difference between the isotope signature at time  $t$  and time zero and where an additional parameter  $\epsilon = 1000(\alpha - 1)$  has been introduced that is called enrichment factor and denoted in permil. Figure

1b shows that for this reaction, eq 7 fits the experimental data very well. Equations 6 and 7 are commonly referred to as Rayleigh equations (19) and are also used for other isotopes (e.g.,  $\delta^2\text{H}$ ,  $\delta^{15}\text{N}$ ,  $\delta^{18}\text{O}$ , etc.) The slope obtained in this case from a linear regression of  $\ln R/R_0$  versus  $\ln f$  is  $-0.0262$  or, if expressed as  $\epsilon$ -value in permil,  $-26.2\%$ . This corresponds to a fractionation factor  $\alpha$  of  $1.000 - 0.026 = 0.974$  (eq 7), meaning that, over the whole time course considered, the <sup>13</sup>CCl<sub>4</sub> molecules consistently reacted by a factor of 0.974 more slowly than the <sup>12</sup>CCl<sub>4</sub> molecules. Consequently, the kinetic isotope effect of this reaction is  $(1/0.974) = 1.027$  (eq 4).

As sketched in Figure 1c, another direct consequence of the isotopic discrimination during the reaction is that the average isotope ratio of all instantaneously formed products is always by the factor  $\epsilon$  isotopically lighter than the ratio of the remaining substrate at the particular point of conversion (see dotted line in Figure 1c). While this instantaneous ratio is not directly observable, the average ratio of all accumulated products can sometimes be measured, which reflects the instantaneous isotopic discrimination only at the beginning of the reaction and is the same as that of the original substrate after complete conversion (see dashed line in Figure 1c). Note, finally, that such a trend is easily recognized, if only one product is formed. If a reaction leads to several products simultaneously, however, their isotope ratios may be very different, and it is only the weighted average of all product ratios that will show the behavior shown in Figure 1c.

**Application of the Rayleigh Equation in Complex Situations.** The main critical question, however, is under which circumstances the Rayleigh equation derived above for a simple molecule such as CCl<sub>4</sub> can be generalized and used to evaluate isotope fractionation in more complex systems (e.g., non-first-order kinetics) and with more complex

molecules (e.g., compounds containing several C-atoms in different locations). Presently, in contaminant hydrology, isotope data are usually presented in form of Rayleigh plots, and reported bulk enrichment factors are generally not easily interpretable in terms of bond-specific rate constants. Nevertheless, in most cases the operational assumption seems to hold reasonably well that the bulk isotope ratio of a small portion of contaminant disappearing in an infinitely short time is consistently by a certain factor different (usually lighter) than that of the remaining substrate. Such correlations are observed even in more complex situations, such as, for example, microbial degradation processes in natural environments. These relationships are of enormous practical value, because if data from microcosm or pure culture experiments are available, it is possible to determine a bulk  $\epsilon$ -value for degradation of a certain contaminant in laboratory experiments, where under controlled conditions and with closed mass balances,  $C/C_0$  and  $\delta^{13}\text{C}$  can be measured at any point of a reaction. In field situations, where it is often difficult to establish mass balances from a limited number of sampling wells, such bulk  $\epsilon$ -values can then be used to assess the extent of in situ biodegradation  $B$  based on the measured isotopic ratios in field samples, according to

$$B = (1 - f) = 1 - \left[ \frac{1000 + \delta^{13}\text{C}_0 + \Delta\delta^{13}\text{C}}{1000 + \delta^{13}\text{C}} \right]^{1000/\epsilon} \quad (8)$$

This approach is sketched in the upper part of Figure 2. As is discussed in detail in recent reviews (12, 24), the applicability of this concept has been demonstrated in an increasing number of cases, and the method is rapidly developing into a powerful tool to monitor natural attenuation at contaminated sites. As a prerequisite, however, the Rayleigh equation must be valid, and in a number of studies it must have been established that the bulk enrichment factor of a certain contaminant is robust and reproducible during degradation under certain conditions. Hence, for a general fundamental understanding of the Rayleigh equation in contaminant hydrology, the following questions are of crucial importance: (a) Is the Rayleigh equation generally valid, also in the case of complex processes involving higher order kinetics and/or slow preceding processes? (b) Does the Rayleigh equation also hold with more complex molecules that contain relevant elements in locations other than the reacting position? (c) How variable are bulk enrichment factors  $\epsilon$  obtained, observed or derived for a given type of reaction, and how can these values be compared if they were determined for different compounds and/or under different conditions? The first aspect is the subject of the next paragraph; the others will be discussed in the following sections.

**Validity of the Rayleigh Equation for Non-First-Order Reactions.** The derivation of the Rayleigh equation above is originally based on the assumption that molecules with light and heavy isotopes react according to first-order rate laws, as expressed in eq 4. It is important to realize, however, that with heavy isotopes of low natural abundance (such as in the case for H, C, N, and O), the Rayleigh equation is also valid for second- and higher-order kinetics. The probability is then very low that two molecules with heavy isotopes are simultaneously engaged in reaction, and as shown in expression (9), the ratio of the corresponding rate equations may be simplified again to an expression analogous to (4)

$$\frac{d({}^h[\text{Substrate}])}{d({}^l[\text{Substrate}])} = \frac{{}^h k({}^h[\text{Substrate}])({}^l[\text{Substrate}])^{(i-1)}}{{}^l k({}^l[\text{Substrate}])({}^l[\text{Substrate}])^{(i-1)}} = \frac{{}^h k({}^h[\text{Substrate}])}{{}^l k({}^l[\text{Substrate}])} \quad (9)$$

where  ${}^l[\text{Substrate}]$  and  ${}^h[\text{Substrate}]$  are substrate molecules of the same compound containing light and heavy isotopes at the reactive site, respectively, and  $i$  is the order of the kinetic rate law. In a second-order reaction with  $i = 2$ , for example, the middle term would be  $\frac{{}^h k({}^h[\text{Substrate}]){}^l[\text{Substrate}]}{{}^l k({}^l[\text{Substrate}])^2}$ , and elimination of  ${}^l[\text{Substrate}]$  in nominator and enumerator would give the term to the right.

In addition, as shown by Melander and Saunders (ref 22; section 10.5) for a Michaelis–Menten model and by Northrop (59) for more general cases, the Rayleigh equation is even applicable if slow steps precede the actual bond conversion and commitment to catalysis is non-negligible such as in many biotransformations. The treatment of such zero- and fractional-order reactions is then given by eq 3 (see above), which expresses that also in these cases a Rayleigh-type behavior may be expected.

**Different Regression Methods.** Recently, there has been a debate about the most adequate way to perform linear regressions such as shown in Figure 1b (63). Regressions in the past were frequently forced through the origin, and many of the  $\epsilon_{\text{bulk}}$  values cited and discussed in this review have been obtained according to this practice. In the case that isotope ratio measurements (e.g., of carbon) are so precise that their error is comparable to the uncertainty of the absolute value of the reference standard, Scott et al. (63) recently suggested using the same formula but refraining from forcing regressions through the origin. We have adopted this practice (e.g., the regression line in Figure 1b has a small offset) and have also applied it to the reevaluation of selected original data in the Excel file of the Supporting Information, part 5. The carbon  $\epsilon_{\text{bulk}}$  values for aerobic MTBE degradation that are recalculated from the original data ( $-1.7$  to  $-2.0\%$ , see “epsilon classical” in the Excel Sheet “Hunkeler et al. Carbon”) are indeed slightly different from the original  $\epsilon_{\text{bulk}}$  values that were obtained by Hunkeler et al. (64) from a regression forced through the origin ( $-1.5$  to  $-2.0\%$ , see Table 3). Similarly, subtle differences are obtained with the original data of Gray et al. (65) (data not shown). Conversely, stronger deviations may be expected if experimental data are associated with a greater uncertainty, as discussed by Scott et al. (63). In this review, literature data from different studies associated with different levels of experimental error are considered. For the sake of clarity, we have chosen to use  $\epsilon_{\text{bulk}}$  values as they were originally published, irrespective of the applied regression method.

### Converting Bulk Enrichment into Apparent Kinetic Isotope Effects (AKIEs)

In most cases in contaminant hydrology, one is dealing with compounds where the isotope of interest may be present in several positions of which only some are reactive. Consequently, many of the isotopes do not directly take part in the reaction, and bulk enrichment factors become smaller due to “dilution” effects from the nonreactive isotopes. Obviously, such enrichment factors no longer directly reflect the underlying fractionation in terms of AKIE values, as was the case in the  $\text{CCl}_4$  example considered above. Hence, to address the meaning and variability of experimental bulk enrichment factors, these  $\epsilon$ -values need to be related to the apparent kinetic isotope effects that can then in turn be compared to the KIE values for well-defined reactions discussed above. Very recently, first approaches have been made toward identifying consistent fractionation patterns, by Morasch et al. with aromatic compounds (66) and by Rudolph et al. with aliphatic hydrocarbons (67, 68). So far however, no general scheme has been proposed that can bridge the gap between the bulk fractionation measured for pollutant transformation and position-specific isotope effects. In the following we suggest an evaluation procedure that corrects for the “trivial”

**TABLE 3. Evaluation of AKIE<sub>c</sub> Values in Established Cases of Microbial Oxidation by Cleavage of a C–H Bond**

carbon kinetic isotope effects expected from the Streitwieser Limit for cleavage of a C–H bond: 1.01–1.02<sup>a</sup>

	ref	ε <sub>bulk</sub>	n <sup>b</sup>	x <sup>b</sup>	ε <sub>reactive position</sub>		Z <sup>b</sup> ε <sub>reactive position</sub>		AKIE		comment	
					true <sup>c</sup>	appr <sup>d</sup>	z <sup>b</sup>	true <sup>c</sup>	appr <sup>d</sup>	true <sup>c</sup>		appr <sup>d</sup>
aerobic biodegradation of MTBE	(65)	–1.5‰ to –1.8‰	5	1	–7.3‰ to –9.9‰	–7.5‰ to –9.0‰	1	–7.3‰ to –9.9‰	–7.5‰ to –9.0‰	1.007–1.010	1.008–1.009	VAFB (aerobic mixed consortium)
aerobic biodegradation of MTBE	(65)	–2.0‰ to –2.4‰	5	1	–9.2‰ to –11.0‰	–10.0‰ to –12.0‰	1	–9.2‰ to –11.0‰	–10.0‰ to –12.0‰	1.009–1.011	1.010–1.012	PM1 (pure aerobic culture)
aerobic biodegradation of MTBE	(64)	–1.5‰ to –2.0‰	5	1	–8.4‰ to –10.0‰	–7.5‰ to –10.0‰	1	–8.4‰ to –10.0‰	–7.5‰ to –10.0‰	1.008–1.010	1.008–1.010	enrichment culture
aerobic biodegradation of <i>tert</i> -butyl alcohol	(64)	–4.2‰	4	3		–5.6‰	3		–16.8‰		1.017	enrichment culture
aerobic biodegradation of 1,2-dichloroethane	(95)	–3.0‰	2	2	–3.0‰		2	–6.0‰		1.006		pure cultures of <i>Pseudomonas sp.</i> strain DCA1
aerobic biodegradation of toluene	(76)	–2.5‰ to –4.2‰	7	1		–17.5‰ to –29.3‰	1		–17.5‰ to –29.3‰		1.018–1.030	<i>Pseudomonas putida</i> , strain <i>mt-2</i> , expts at varying temp
anaerobic biodegradation of toluene	(15, 76)	–1.7‰ to –1.8‰	7	1		–11.9‰ to –12.6‰	1		–11.9‰ to –12.6‰		1.012–1.013	sulfate-, iron-, and nitrate reducing pure cultures
anaerobic biodegradation of toluene	(75)	–0.5‰ to –0.8‰	7	1		–3.5‰ to –5.6‰	1		–3.5‰ to –5.6‰		1.004–1.006	sulfate-reducing and methanogenic enrichment cultures
anaerobic biodegradation of <i>m</i> -cresol	(66)	–3.9‰	7	1		–27.3‰	1		–27.3‰		1.028	sulfate-reducing culture
anaerobic biodegradation of <i>p</i> -cresol	(66)	–1.6‰	7	1		–11.2‰	1		–11.2‰		1.011	sulfate-reducing culture
anaerobic biodegradation of 2-methylnaphthalene	(99)	–0.9‰	11	1		–9.9‰	1		–9.9‰		1.010	sulfate-reducing enrichment culture
anaerobic biodegradation of <i>o</i> -xylene	(66)	–1.5‰	8	2		–6.0‰	2		–12.0‰		1.012	sulfate-reducing culture
anaerobic biodegradation of <i>m</i> -xylene	(66)	–1.8‰	8	2		–7.2‰	2		–14.4‰		1.015	sulfate-reducing culture

<sup>a</sup> Approximate estimate from Streitwieser Limit (see Table 1). <sup>b</sup> n: number of atoms of the element considered that are present in the molecule; x of them are located at the reactive site; z of which are in intramolecular isotopic competition. <sup>c</sup> Correctly evaluated analogous to eqs 14/15. <sup>d</sup> Approximated by ε<sub>reactive position</sub> ≈ n/x·ε<sub>bulk</sub> (eq 16).



aspects which distort the magnitude of bulk  $\epsilon$ -values determined by CSIA: (i) the presence of heavy isotopes in nonreactive positions of a molecule. They “dilute” the isotope fractionation at the reactive position leading to much smaller observable changes in the average bulk isotopic signature. (ii) The simultaneous presence of heavy and light isotopes in indistinguishable, reactive positions of the same molecule. Due to intramolecular competition between the equivalent sites, reaction of the heavy isotopes is to a great part circumvented. Although both corrections will be introduced in an illustrative way, it should be emphasized that they are really the outcome of a quite general mathematical derivation that starts off from the fundamental rate laws that underlie the Rayleigh equation, leading directly to the corresponding equations (see the Supporting Information). These equations apply for any element with heavy isotopes of low natural abundance (H, C, N, O, but not S, Cl).

**Correction for Nonreactive Locations.** A correction for nonreactive locations is straightforward as illustrated by the following example. We consider the microbial transformation of methyl *tert*-butyl ether (MTBE) under aerobic conditions. In this scenario the postulated initial reaction is the oxidative cleavage of a C–H bond at the methyl group (see pathway (1) in Scheme 1). For this reaction, both  $\delta^{13}\text{C}$  as well as  $\delta^2\text{H}$  data have been collected, and bulk  $\epsilon$ -values derived from these data have been reported in the literature (Tables 3 and 4). We first consider the  $\delta^{13}\text{C}$  values, for which the changes  $\Delta\delta^{13}\text{C}$  must be corrected with respect to nonreactive locations. Considering an evenly distributed substrate pool at the beginning of the reaction where the heavy isotopes are of low natural abundance, only one out of five  $^{13}\text{C}$ -containing MTBE molecules will have  $^{13}\text{C}$  in the methyl group and react more slowly than pure  $^{12}\text{C}$ -MTBE, thus leading to isotope fractionation:

$$\frac{-d[^{13}\text{CH}_3\text{-O-C}_4\text{H}_9]}{-d[\text{CH}_3\text{-O-C}_4\text{H}_9]} = \alpha_{\text{reactive position}} \cdot \frac{[^{13}\text{CH}_3\text{-O-C}_4\text{H}_9]}{[\text{CH}_3\text{-O-C}_4\text{H}_9]} \quad (10)$$

Conversely, reaction of the other four out of five  $^{13}\text{C}$ -containing MTBE molecules, which have  $^{13}\text{C}$  in the nonreacting *tert*-butyl group, will *not* lead to fractionation, as isotopes are too far away from the reacting bond to make a difference:

$$\frac{-d[\text{CH}_3\text{-O-}^{13}\text{CC}_3\text{H}_9]}{-d[\text{CH}_3\text{-O-C}_4\text{H}_9]} = 1 \cdot \frac{[\text{CH}_3\text{-O-}^{13}\text{CC}_3\text{H}_9]}{[\text{CH}_3\text{-O-C}_4\text{H}_9]} \quad (11)$$

Therefore, if the bulk isotope ratio is analyzed, the changes in this *average* ratio will be much smaller than those at the reactive location. Moreover, because the molecules exhibiting a  $^{13}\text{C}$ -atom at the methyl group react more slowly than the molecules exhibiting a  $^{13}\text{C}$ -atom in the *tert*-butyl group, the former tend to accumulate with respect to the latter during the course of the reaction. Hence, the proportion of molecules that lead to fractionation increases with time, and if average bulk isotope ratios are measured with GC–IRMS, it will seem that it is actually the fractionation that increases over the reaction (see the Supporting Information, part 4). Most traditional evaluations of average bulk isotope ratios can, therefore, not even be expected to follow the Rayleigh model, because a plot according to eq 7 should lead to nonlinear regressions with an upward curvature. The fact that this effect has never been observed indicates that the expected accumulation is generally irrelevant within the analytical precision and that bulk enrichment factors give valuable descriptive parameters for practical purposes. Plots with a “true” Rayleigh behavior, however, that lead to position-specific enrichment factors with a physical meaning (i.e.,

interpretable in terms of reaction rate constants) can only be expected either (1) with symmetric molecules where all positions are potentially reactive (e.g.,  $\text{CCl}_4$ , or 1,2-dichloroethane,  $\text{CH}_2\text{Cl-CH}_2\text{Cl}$ , as well as benzene,  $\text{C}_6\text{H}_6$ ) or (2) after an appropriate correction for the nonreacting locations. As shown in the mathematical derivation in the Supporting Information, such a correction can be achieved by converting changes in the bulk isotopic signature  $\Delta\delta^{13}\text{C}_{\text{bulk}}$  into changes in the position-specific isotopic signature at the reacting methyl group  $\Delta\delta^{13}\text{C}_{\text{reactive position}}$ , for example in the case of MTBE oxidation:

$$\Delta\delta^{13}\text{C}_{\text{reactive position}} = (5/1) \cdot \Delta\delta^{13}\text{C}_{\text{bulk}} \quad (12)$$

Similarly, for hydrogen fractionation, where 3 out of 12 atoms are located at the reacting methyl group, the correction is

$$\Delta\delta^2\text{H}_{\text{reactive position}} = (12/3) \cdot \Delta\delta^2\text{H}_{\text{bulk}} \quad (13)$$

**The Effect of Intramolecular Isotope Distributions.** In both cases it is assumed that initially the isotopes are distributed evenly over the whole molecule. A review of published intramolecular isotope ratios in the Supporting Information, part 5, provides evidence that this approximation is not exactly true but that some deviations between different molecular positions do exist. Generally these variations are (a) greater in manmade than in natural compounds and (b) significantly greater for hydrogen (typically  $\pm 20\%$ , extreme cases  $+100\%/ -50\%$ ) than for heavier elements such as carbon (typically  $\pm 1-2\%$ , extreme deviations  $\pm 5\%$ ). Although it may not be commonly realized, even simple comparisons of published  $\epsilon_{\text{bulk}}$  values from different laboratories rely, therefore, on the silent assumption that isotopes are evenly distributed inside the investigated compounds. Considering the uncertainty introduced by this approximation, an error propagation shows that with an intramolecular isotope variation of  $\pm 5\%$  (this would correspond to an extreme scenario in the case of carbon), the relative error in  $\epsilon_{\text{reactive position}}$  would also be 5% (e.g., 1‰ in the case of  $\epsilon_{\text{reactive position}} = -20\%$ , and 5‰ in the case of  $\epsilon_{\text{reactive position}} = -100\%$ , etc.). These relatively small deviations illustrate that with heavy elements such as carbon, the working hypothesis of a random isotope distribution is usually reasonable, whereas in the case of hydrogen these isotope variations may occasionally become important. As shown in the Supporting Information, part 2, our correction for nonreactive locations provides for the first time the context to understand this artifact and to take it into account: When knowing the initial isotopic distribution (e.g., in the case of carbon from analysis of compound fragments by GC–IRMS (69–71) or in the case of hydrogen from SNIF-NMR (Site-Specific Natural Isotope Fractionation by Nuclear Magnetic Resonance Spectroscopy) measurements (72)) the factors 5/1 and 12/3 can easily be replaced using the measured distributions, and unbiased  $\epsilon_{\text{reactive position}}$  values may be calculated.

**Calculation of Position-Specific Enrichment Factors.** Insertion of the approximation made by eqs 12 and 13, respectively, in the corresponding Rayleigh equation (eq 7 and analogue equation for  $\delta^2\text{H}$ ) yields for oxidation of MTBE

$$\ln \frac{R}{R_0} = \ln \frac{(1000 + \delta^{13}\text{C}_0 + 5\Delta\delta^{13}\text{C}_{\text{bulk}})}{(1000 + \delta^{13}\text{C}_0)} = \frac{\epsilon_{\text{reactive position}}^{\text{C}}}{1000} \cdot \ln f \quad (14)$$

and



$$\ln \frac{R}{R_0} = \ln \frac{(1000 + \delta^2H_0 + 4\Delta\delta^2H_{\text{bulk}})}{(1000 + \delta^2H_0)} = \frac{\epsilon_{\text{reactive position}}^{\text{H}}}{1000} \cdot \ln f \quad (15)$$

Tables 3 and 4 give the  $\epsilon_{\text{reactive position}}^{\text{C}}$  and  $\epsilon_{\text{reactive position}}^{\text{H}}$  values derived from a reevaluation (linear regression of eqs 14 and 15, respectively) of the original data provided by Jennifer McKelvie (Gray) (65). Also given are approximated values not using the original data but only the reported  $\epsilon_{\text{bulk}}$  values

$$\epsilon_{\text{reactive position}} \approx n/x \cdot \epsilon_{\text{bulk}} \quad (16)$$

where  $n$  is the number of the atoms of the element considered of which  $x$  are located at the reactive site, in this case the methyl group. Hence, for carbon,  $n = 5$  and  $x = 1$ , whereas for hydrogen,  $n = 12$  and  $x = 3$ . As can be seen from Tables 3 and 4, for carbon, the approximated  $\epsilon_{\text{methyl}}$  values are quite close to the values derived from the original data, while for hydrogen, the deviations are more pronounced. Nevertheless, if only  $\epsilon_{\text{bulk}}$  values are available, eq 16 can be used to approximate  $\epsilon$ -values for any reactive position with reasonable accuracy. A justification of eq 16 as well as a more detailed characterization of the systematic error associated with its use is given in the Supporting Information, part 4. It is shown that in the case of carbon isotopes, the approximated  $\epsilon_{\text{reactive position}}$  overestimates the true value by up to 15% (i.e., 12.3‰) for the scenario  $\text{AKIE}_{\text{C}} = 1.09$ ,  $n/x = 8$  and an evaluation down to  $\ln f = -4$ . Likewise, it is shown how the systematic error can become 100% and greater in the case of hydrogen isotopes.

If there is only one reactive position in the molecule, an apparent kinetic isotope effect (AKIE) for this position and element can directly be calculated (see also eq 2):

$$\text{AKIE}_{\text{E}} = \frac{\left(\frac{k}{h k}\right)_{\text{apparent}}}{\alpha_{\text{reactive position}}} = \frac{1}{\frac{1}{1 + \epsilon_{\text{reactive position}}/1000}} \quad (17)$$

This is the case for the oxidation of the methyl carbon in MTBE ( $\text{AKIE}_{\text{C}}=1.01$ , Table 3) as well as for the reduction of the carbon in  $\text{CCl}_4$  by the iron porphyrin (see above), for which a larger  $\text{AKIE}_{\text{C}}$  value of 1.027 is obtained. We will come back to these values later when discussing the transformation of the two compounds under various conditions.

**Intramolecular Isotopic Competition.** In contrast to the methyl carbon, for the methyl hydrogens in MTBE, an additional correction has to be made in order to derive an appropriate AKIE value. In this case, there is not only *intermolecular* isotopic competition between light (i.e.,  $-\text{CH}_3$ ) and heavy (i.e.,  $-\text{CDH}_2$ ) methyl groups of different molecules but also *intramolecular* competition between the two hydrogens and the deuterium present in the same methyl group. In the absence of masking, this intramolecular competition can be taken into account by writing  $\alpha_{\text{reactive position}}$  in terms of the relevant rate constants (for a more general discussion including commitment to catalysis see the Supporting Information, part 2)

$$\frac{-d[\text{CH}_2\text{D-}]/dt}{-d[\text{CH}_3\text{-}]/dt} = \alpha_{\text{reactive position}} \cdot \frac{[\text{CH}_2\text{D-}]}{[\text{CH}_3\text{-}]} = \frac{2 \cdot {}^1k + {}^2k}{3 \cdot {}^1k} \cdot \frac{[\text{CH}_2\text{D-}]}{[\text{CH}_3\text{-}]} \quad (18)$$

and therefore

**TABLE 4. Evaluation of  $\text{AKIE}_{\text{H}}$  Values in Established Cases of Microbial Oxidation by Cleavage of a C–H Bond<sup>e</sup>**

ref	$\epsilon_{\text{bulk}}$	$n^b$	$x^b$	$\epsilon_{\text{reactive position}}$		$z^c$	$z \cdot \epsilon_{\text{reactive position}}$		comment
				true <sup>c</sup>	appr <sup>d</sup>		true <sup>c</sup>	appr <sup>d</sup>	
aerobic biodegradation of MTBE (65)	-29‰/-66‰	12	3	-136‰/-202‰	-116‰/-264‰	3	-408‰/-606‰	-348‰/-792‰	1.53/4.81 VAFB (aerobic mixed consortium)
aerobic biodegradation of MTBE (65)	-33‰ to -37‰	12	3	-137‰	-132‰ to -148‰	3	-411‰	-396‰ to -444‰	1.66–1.80 PM1 (pure aerobic culture)
anaerobic biodegradation of toluene (126)	-12‰ to -65‰ <sup>e</sup>	8	3	-927‰ to -956‰	-32‰ to -173‰	3	-927‰ to -956‰	-96‰ to -520‰	1.1 to 2.1 mixed methanogenic consortium
aerobic biodegradation of toluene (76, 127)	-927‰ to -956‰			-927‰ to -956‰			-927‰ to -956‰		<i>Pseudomonas putida</i> , experiments with labeled substrate
anaerobic biodegradation of toluene (76, 127)	-514‰ to -735‰			-514‰ to -735‰			-514‰ to -735‰		sulfate-, iron- and nitrate reducing pure cultures, expts with labeled substrate

<sup>a</sup> Typical range of values (see Table 2). <sup>b</sup>  $n$ : number of atoms of the element considered that are present in the molecule;  $x$  of them are located at the reactive site;  $z$  of which are in intramolecular isotopic competition. <sup>c</sup> Correctly evaluated analogous to eqs 14/15. <sup>d</sup> Approximated by  $\epsilon_{\text{reactive position}} \approx n/x \cdot \epsilon_{\text{bulk}}$  (eq 16). <sup>e</sup> Italic numbers indicate values outside the typical range.

$$\frac{\epsilon_{\text{reactive position}}}{1000} = \alpha_{\text{reactive position}} - 1 = \frac{1}{3} \dots \dots \dots \left. \right) \quad (19)$$

which yields

$$\text{AKIE}_{\text{H}} = \left( \frac{{}^1k}{{}^2k} \right)_{\text{apparent}} = \frac{1}{1 + 3 \cdot \epsilon_{\text{reactive position}} / 1000} \quad (20)$$

Note that secondary isotope effects due to the presence of deuterium adjacent to a broken C–H bond have been neglected (i.e., the  ${}^1k$  values for oxidation of  $\text{CH}_2\text{D}$ – and  $\text{CH}_3$ – have been assumed equal). As secondary isotope effects are considerably smaller than the primary effects caused by the actual bond cleavage (47), this approximation seems reasonable (only if both effects are large, eq 20 will eventually lead to negative AKIE values so that the correct equation (S34) in the Supporting Information must then be used). However, particularly in the case of hydrogen, secondary isotope effects can, of course, not be neglected if primary effects are absent. We will address such a case later when discussing the microbial transformation of MTBE under anaerobic conditions.

It is important to realize, finally, that in the case of symmetric molecules such as 1,2-dichloroethane ( $\text{CH}_2\text{Cl}$ – $\text{CH}_2\text{Cl}$ ) or benzene ( $\text{C}_6\text{H}_6$ ) it is still necessary to perform a correction for intramolecular competition, whereas no correction for nonreactive positions needs to be made, because all atoms are in equivalent, reactive positions (ref 22, chapter 4). Expression 20 can be generalized for any element with isotopes of low natural abundance if intramolecular competition between  $z$  indistinguishable, reactive sites exists:

$$\text{AKIE}_{\text{E}} = \left( \frac{{}^1k}{{}^h k} \right)_{\text{apparent}} = \frac{1}{1 + z \cdot \epsilon_{\text{reactive position}} / 1000} \quad (21)$$

In the case of molecules such as 1,2-dichloroethane ( $\text{CH}_2\text{Cl}$ – $\text{CH}_2\text{Cl}$ )  $\epsilon_{\text{reactive position}}$  is then simply obtained from the traditional application of the Rayleigh equation. (As a consequence,  $\epsilon_{\text{reactive position}}$  values of symmetric molecules that are reported in Tables 3–8 are not approximate, but exact values, because the Rayleigh evaluation of the original papers was the appropriate evaluation in these cases.) In the case of molecules with nonreacting positions, however,  $\epsilon_{\text{reactive position}}$  must be derived from the original isotope signature data as shown above (e.g., eqs 14 and 15 for carbon and hydrogen, respectively) or approximated from  $\epsilon_{\text{bulk}}$  values (eq 16). Note that in this latter case, because for primary isotope effects  $z = x$ , the AKIE value may be approximated by (only for primary isotope effects in nonconcerted reactions):

$$\text{AKIE}_{\text{E}} \approx \frac{1}{1 + n \cdot \epsilon_{\text{bulk}} / 1000} \quad (22)$$

For most of the following examples, only approximate  $\epsilon_{\text{reactive position}}$  and corresponding AKIE values are used, because, in the literature, only  $\epsilon_{\text{bulk}}$  and not the original isotope data are commonly reported. Note that the term  $n \cdot \epsilon_{\text{bulk}}$  in eq 22 is equivalent to the parameter  $\epsilon_{\text{intrinsic}}$  that was recently introduced by Morasch et al. (66) as a means to take into account the number of total carbon atoms inside contaminants. Values of  $\epsilon_{\text{intrinsic}}$  or  $n \cdot \epsilon_{\text{bulk}}$  are not easily interpretable, however, if reactions are concerted (see rule of thumb no. 6) or if secondary rather than primary isotope effects are observed (for a treatment of secondary isotope effects see later in this review). Also, these parameters cannot take into account the effect of an uneven intramolecular isotope distribution.

The main features of our evaluation scheme are summarized again in Figure 2. The top part sketches the “traditional” evaluation of  $\epsilon_{\text{bulk}}$  values and their application in the field. The lower left part illustrates how the new correction for nonreactive locations (eqs 12 and 13) gives changes of isotope ratios directly in the reactive position. If these values are inserted in the Rayleigh equation, position-specific enrichment factors  $\epsilon_{\text{reactive position}}$  may be calculated (eqs 14 and 15). Using such  $\epsilon_{\text{reactive position}}$  values and applying the correction for intramolecular competition (eq 21), apparent kinetic isotope effects (AKIE values) are obtained. (Alternatively,  $\epsilon_{\text{reactive position}}$  and AKIE values may be obtained by the approximate eqs 16 and 22.) The lower right part of Figure 2 gives an outlook on the next section, where AKIE values will be compared to published KIE data so that mechanistic information about transformation pathways can be obtained.

### Evaluation of Published Isotope Fractionation Data in Terms of AKIE Values

The transformation of bulk isotope fractionation data into position-specific apparent kinetic isotope effects (AKIE) provides a number of advantages. For the same known chemical reaction (e.g., oxidation of a C–H bond), isotope fractionation can be compared in different, structurally very dissimilar contaminants, irrespective of their molecular size. Common fractionation trends can thus be established, and in cases where AKIE and expected KIE differ significantly, this insight might even be used to infer underlying reasons such as the presence of slow, nonfractionating steps (situations of commitment to catalysis). In the following such fractionation patterns are discussed for reactions of well-defined degradation pathways, namely for the oxidation of alkyl groups, for  $\text{S}_{\text{N}}2$  reactions, for reductive dissociation of C–Cl bonds and for oxidation at double bonds. Alternatively, if transformation can occur in several ways and the mechanism is yet uncertain, the evaluation procedure can be performed under the assumption of different degradation scenarios. Depending on which bond of the molecule is assumed to be involved, appropriate numbers of  $n$ ,  $x$ , and  $z$  may be chosen, and a hypothetical AKIE can be calculated in each case. Calculated AKIE and expected KIE can then be compared for each reaction, and degradation scenarios can be confirmed or discarded (see sketch in the lower right part of Figure 2). This will be illustrated for the anaerobic degradation of MTBE and the aerobic degradation of 1,2-dichloroethane. It is demonstrated how such an analysis is even possible if slow steps lead to AKIE values that are much smaller than expected KIE values, provided that isotope fractionation is measured for two elements simultaneously. The calculation of AKIE values is difficult, however, if a well-understood transformation hypothesis does not exist and KIE reference data are not available such as with anaerobic benzene degradation (73) and dehalogenation of polychlorinated benzenes (74). As discussions would remain speculative at this point, these compounds are not included in the following section.

**Oxidation at Saturated Carbon Atoms.** The first type of reaction considered is the oxidative cleavage of C–H bonds as encountered in the aerobic degradation of MTBE, 1,2-dichloroethane, and in both the aerobic and anaerobic oxidation of aromatic methyl groups (Tables 3 and 4). For all three cases, the carbon AKIE are within the range of  $\text{AKIE}_{\text{C}} = 1.004$ – $1.030$  consistent with the estimate based on Streitwieser Limits as well as the value reported from one study for cleavage of a C–H bond (see Tables 1 and 2). The somewhat smaller values including  $\text{AKIE}_{\text{C}} = 1.004$ – $1.006$  for the anaerobic toluene degradation by mixed microbial cultures (75) or  $\text{AKIE}_{\text{C}} = 1.006$  for the aerobic oxidation of 1,2-dichloroethane (95) may be an indication that steps other

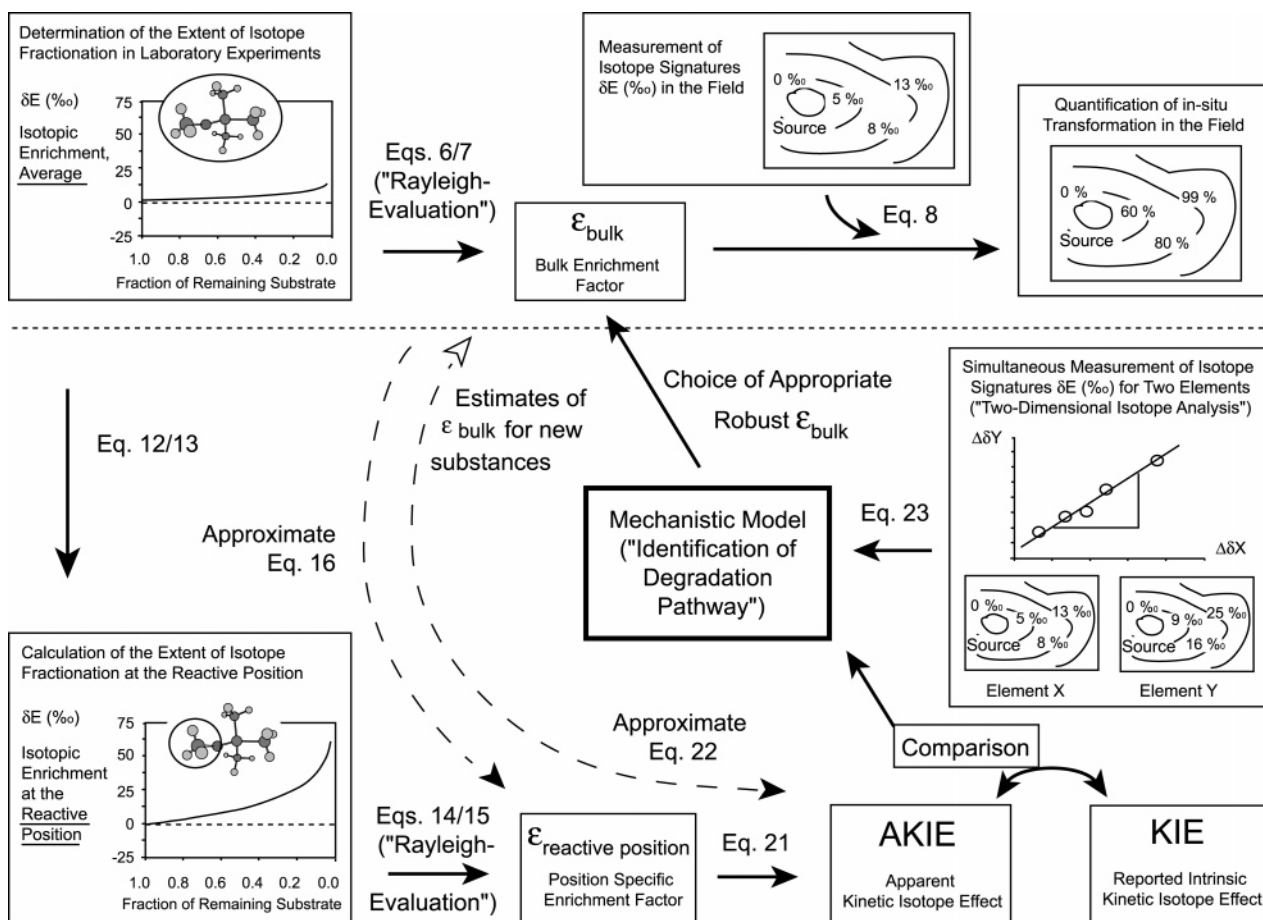


**FIGURE 2.** Main features of the evaluation scheme of this review. The upper part represents conventional applications of the Rayleigh equation. The lower part sketches how our corrections for nonreacting locations (eqs 12/13/14/15) and intramolecular competition (eq 21) lead to AKIE values that may be used to establish appropriate enrichment factors and infer transformation pathways.

than the actual bond cleavage (e.g., transport and binding to the enzymatic site, substrate activation in intermediate enzyme complexes, etc.) were also rate-determining. Conversely, cases of very large fractionation such as  $AKIE_C = 1.030$  in aerobic degradation of toluene with *Pseudomonas putida mt-2* (76) or  $AKIE_C = 1.028$  in anaerobic degradation of *m*-cresol with *Desulfobacterium cetonicum* (66) imply that C–H bond cleavage was the dominant rate-limiting step in these transformations. The hydrogen data reported in a few studies also yield  $AKIE_H$  values (2–23) that are typical for cleavage of an H-bond (Table 4). The large  $AKIE_H$  of 14–23 for the aerobic degradation of toluene with *P. putida mt-2* (76) confirms that the C–H bond cleavage must have been the rate-determining step in this reaction. Conversely, the rather small  $AKIE_H$  of 1.7–2.5 derived for the aerobic degradation of MTBE (65) may again be indicative of slow nonfractionating steps preceding the isotopically sensitive bond cleavage.

**$S_N2$  Type Reactions.** Compared to oxidation reactions involving C–H cleavage, the carbon isotope effects obtained from reevaluation of  $S_N2$  reactions are consistently much larger with  $AKIE_C$  values generally between 1.029 and 1.072 (Table 5). These results are again in good agreement with KIE values for  $S_N2$  reactions reported in the chemical literature (1.03–1.09, Table 2). The higher values reflect partly the fact that carbon atoms are now bound to an atom (e.g., Cl, Br) that is much heavier than H. Partly they also arise because  $S_N2$  reactions are special in that they show a maximum isotope effect already at realistic “average” transition states of about 50% bond changes rather than hypothetically late transition states (see “rules of thumb” above). Note that there is no

consistent difference between the isotope effects in abiotic vs biotic  $S_N2$  reactions. This reflects the general fact that isotope effects are primarily indicative of the *type* of degradation reaction, irrespective of its abiotic or enzymatic character. If the same bond is broken in the same way, then a similar intrinsic isotope effect can be expected; however, this value may again be masked by slow nonfractionating preceding processes. For example, for the degradation of methylbromide by the bacterial strain CC495 (77), the small  $AKIE_C$  obtained may be due to partly rate-limiting step(s) preceding the transformation of the compound. The low values obtained with assays of isolated enzyme in the case of methyl chloride suggest that it is not only the transfer through the cell membrane that may be rate-limiting but that also an elevated commitment to catalysis (e.g., secondary slow steps in the actual enzyme reaction) occurred.

**Oxidation of C–C Double Bonds.** In both the reaction of alkenes with permanganate and in epoxidation reactions one can assume a concerted mechanism meaning that  $n = 2$ ,  $x = 2$ , and  $z = 1$ : both positions of the double bond are simultaneously involved in the reaction, but no intramolecular competition takes place (50, 58). The calculated  $AKIE_C$  for oxidation of chlorinated ethenes by permanganate is in the range of  $AKIE_C = 1.016–1.028$  (Table 6), which is in good agreement with the reference value of  $KIE_C = 1.024$  reported by Houk and co-workers (58) (see Table 2). In the case of *microbial* oxidation of substituted ethenes, which occurs probably by epoxidation (78), much smaller values of 1.001, 1.000, and 1.003–1.008 are calculated for trichloroethene (TCE), *cis*-dichloroethene (*cis*-DCE), and vinyl chloride (VC) (see Table 7). For VC, the values are again comparable to the

**TABLE 5. Evaluation of AKIE<sub>C</sub> Values in Established Cases of Second-Order Nucleophilic Substitution Reactions (S<sub>N</sub>2-Type)<sup>g</sup>**

carbon kinetic isotope effects KIE reported in the classical literature: 1.03–1.09<sup>a</sup>

	ref	ε <sub>bulk</sub>	n <sup>b</sup>	x <sup>b</sup>	ε <sub>reactive position</sub>		Z · ε <sub>reactive position</sub>		AKIE		comment
					true <sup>c</sup>	appr <sup>d</sup>	z <sup>b</sup>	true <sup>c</sup>	appr <sup>d</sup>	true <sup>c</sup>	
abiotic reaction of methyl bromide to methyl chloride	(128)	-41.5‰	1	1	-41.5‰		1	-41.5‰	1.043		abiotic transhalogenation of CH <sub>3</sub> Br in the presence of Cl <sup>-</sup>
abiotic degradation of methyl bromide	(129)	-56‰ <sup>e</sup>	1	1	-56‰		1	-56‰	1.059		reaction in sterile soil microcosms
aerobic biodegradation of dichloromethane	(14)	-42.4‰ <sup>f</sup>	1	1	-42.4‰		1	-42.4‰	1.044		pure culture (MC8b)
aerobic biodegradation of methyl chloride	(77, 129)	-42‰ to -48‰ <sup>e</sup>	1	1	-42‰ to -48‰		1	-42‰ to -48‰	1.044 to 1.050		pure cultures (IMB-1) and (MB-2), soil microcosms
aerobic biodegradation of methyl bromide	(77, 129)	-54‰ to -67‰ <sup>e</sup>	1	1	-54‰ to -67‰		1	-54‰ to -67‰	1.057 to 1.072		pure cultures (IMB-1) and (MB-2), soil microcosms
aerobic biodegradation of methyl iodide	(77)	-28‰ to -38‰ <sup>e</sup>	1	1	-28‰ to -38‰		1	-28‰ to -38‰	1.029 to 1.040		pure cultures (IMB-1) and (MB-2)
aerobic biodegradation of methyl chloride, bromide, and iodide	(77)	-4‰ to -40‰ <sup>e</sup>	1	1	-4‰ to -40‰		1	-4‰ to -40‰	1.004 <sup>g</sup> to 1.042		pure culture (CC495), enzyme isolated from CC495
aerobic biodegradation of 1,2-dichloroethane	(17, 95)	-27‰ to -33‰	2	2	-27‰ to -33‰		2	-54‰ to -66‰	1.057 to 1.068		pure cultures of <i>X. autotrophicus</i> GJ10 and <i>A. aquaticus</i> AD20

<sup>a</sup> Typical range of values (see Table 2). <sup>b</sup> n: number of atoms of the element considered that are present in the molecule; x of them are located at the reactive site; z of which are in intramolecular isotopic competition. <sup>c</sup> Correctly evaluated analogous to eqs 14/15. <sup>d</sup> Approximated by ε<sub>reactive position</sub> ≈ n/x·ε<sub>bulk</sub> (eq 16). <sup>e</sup> Calculated from reported AKIE (note that the way in which ε-values are defined in ref 77 gives these data the meaning (AKIE-1), as expressed in permil). <sup>f</sup> Calculated from reported α-values. <sup>g</sup> Italic numbers indicate values outside the typical range.

**TABLE 6. Evaluation of AKIE<sub>C</sub> Values for Oxidation of a Double Bond with Permanganate**

carbon isotope effect reported in the literature (per carbon atom): 1.024<sup>a</sup>

	ref	ε <sub>bulk</sub>	n <sup>b</sup>	x <sup>b</sup>	ε <sub>reactive position</sub>		Z · ε <sub>reactive position</sub>		AKIE	
					true <sup>c</sup>	appr <sup>d</sup>	z <sup>b</sup>	true <sup>c</sup>	appr <sup>d</sup>	true <sup>c</sup>
degradation of tetrachloroethene with permanganate	(130)	-15.7‰ to -17.7‰ <sup>e</sup>	2	2	-15.7‰ to -17.7‰		1	-15.7‰ to -17.7‰	1.016 to 1.018	
degradation of trichloroethene with permanganate	(13, 133)	-18.5‰ to -26.8‰ <sup>e</sup>	2	2	-18.5‰ to -26.8‰		1	-18.5‰ to -26.8‰	1.019 to 1.028	
degradation of <i>cis</i> -dichloroethene with permanganate	(130)	-21.1‰ <sup>e</sup>	2	2	-21.1‰		1	-21.1‰	1.022	

<sup>a</sup> Reported literature value (see Table 2). <sup>b</sup> n: number of atoms of the element considered that are present in the molecule; x of them are located at the reactive site; z of which are in intramolecular isotopic competition; here, z = 1, because reaction is concerted. <sup>c</sup> Correctly evaluated analogous to eqs 14/15. <sup>d</sup> Approximated by ε<sub>reactive position</sub> ≈ n/x·ε<sub>bulk</sub> (eq 16). <sup>e</sup> Calculated from reported α-values;

**TABLE 7. Evaluation of AKIE<sub>C</sub> Values for Epoxidation of a Double Bond<sup>e</sup>**

carbon isotope effect reported in the literature (per carbon atom): 1.011<sup>a</sup>

	ref	ε <sub>bulk</sub>	n <sup>b</sup>	x <sup>b</sup>	ε <sub>reactive position</sub>		Z · ε <sub>reactive position</sub>		AKIE		comment
					true <sup>c</sup>	appr <sup>d</sup>	z <sup>b</sup>	true <sup>c</sup>	appr <sup>d</sup>	true <sup>c</sup>	
aerobic biodegradation of vinyl chloride	(79, 131)	-3.2‰ to -8.2‰	2	2	-3.2‰ to -8.2‰		1	-3.2‰ to -8.2‰	1.003 <sup>e</sup> to 1.008		various pure metabolic and cometabolic cultures
aerobic biodegradation of <i>cis</i> -dichloroethene	(79)	-0.4‰	2	2	-0.4‰		1	-0.4‰	1.000 <sup>e</sup>		cometabolic culture <i>Methylosinus</i>
trichloroethene		-1.1‰	2	2	-1.1‰		1	-1.1‰	1.001 <sup>e</sup>		<i>trichosporium</i> OB3b
aerobic biodegradation of trichloroethene	(80)	-18.2‰ to -20.7‰	2	2	-18.2‰ to -20.7‰		1	-18.2‰ to -20.7‰	1.019 to 1.021 <sup>e</sup>		pure culture <i>Burkholderia Cepacia</i> G4

<sup>a</sup> Reported literature value (see Table 2). <sup>b</sup> n: number of atoms of the element considered that are present in the molecule; x of them are located at the reactive site; z of which are in intramolecular isotopic competition; here, z = 1, because reaction is concerted. <sup>c</sup> Correctly evaluated analogous to eqs 14/15. <sup>d</sup> Approximated by ε<sub>reactive position</sub> ≈ n/x·ε<sub>bulk</sub> (eq 16). <sup>e</sup> Italic numbers indicate values outside the typical range.

reference KIE<sub>C</sub> = 1.011 that was measured for chemical epoxidation by *m*-Cl perbenzoic acid (50) (see Table 2). Conversely, the lower values for TCE and *cis*-/*trans*-DCE as reported by Chu et al. (79) suggest substantial commitment to catalysis. The very large fractionation (AKIE<sub>C</sub> = 1.019–1.021) that has been reported for aerobic biodegradation of TCE in an earlier study (80) does not seem to be consistent with such an epoxidation mechanism, indicating that a different degradation mechanism may have prevailed in this study.

**Reduction of C–Cl Bonds.** A number of studies have investigated isotope fractionation during reductive dechlorination of chlorinated hydrocarbons by biotic and abiotic processes. Typical AKIE<sub>C</sub> values for the reductive cleavage of C–Cl bonds have been reported in a recent study on the reductive dehalogenation of CCl<sub>4</sub> at different Fe(II) bearing mineral surfaces, where it may be assumed that surface sorption/desorption of CCl<sub>4</sub> molecules at the surface is fast (81). All AKIE<sub>C</sub> values obtained with nonsulfidic minerals were in the range of 1.027–1.033 (Table 8), corresponding



**TABLE 8. Evaluation of AKIE<sub>C</sub> Values in Established Cases of Reduction by Cleavage of One C–Cl Bond<sup>e</sup>**

	carbon kinetic isotope effect expected from the Streitwieser Limit for cleavage of a C–Cl bond: $\approx 1.03^a$											
	ref	$\epsilon_{\text{bulk}}$	$n^b$	$x^b$	$\epsilon_{\text{reactive position}}$		$z^b$	$Z \cdot \epsilon_{\text{reactive position}}$		AKIE		comment
					true <sup>c</sup>	appr <sup>d</sup>		true <sup>c</sup>	appr <sup>d</sup>	true <sup>c</sup>	appr <sup>d</sup>	
reduction of CCl <sub>4</sub> by Fe(II) on iron oxides and other abiotic reductands	(62) (81)	–26‰ to –32‰	1	1	–26‰ to –32‰		1	–26‰ to –32‰		1.027 to 1.033		abiotic reductands including Fe(II) on different iron(II) oxides, Fe(II) porphyrin
reduction of CCl <sub>4</sub> by mackinawite (FeS)	(81)	–16‰			–16‰			–16‰		1.016 <sup>e</sup>		different syntheses of mackinawite
reduction of tetrachloroethene by vitamin B12	(85)	–15.8‰/ –16.5‰	2	2	–15.8‰/ –16.5‰		2	–31.6‰/ –33‰		1.033/ 1.034		
microbial reduction of tetrachloroethene	(16) (87)	–2‰ to –5.5‰	2	2	–2‰ to –5.5‰		2	–4‰ to –11‰		1.004 <sup>e</sup> to 1.011 <sup>e</sup>		different mixed consortia including KB-1, field data
reduction of trichloroethene by vitamin B12	(85)	–16.6‰/ –17.2‰	2	1	–33.2‰/ –34.4‰		1	–33.2‰/ –34.4‰		1.034/ 1.036		
microbial reduction of trichloroethene	(13) (16) (86) (87)	–2.5‰ to –13.8‰	2	1	–5‰ to –27.6‰		1	–5‰ to –28‰		1.005 <sup>e</sup> to 1.028		different mixed consortia including KB-1, field data

<sup>a</sup> Approximate estimate from Streitwieser Limit (see Table 1). <sup>b</sup>  $n$ : number of atoms of the element considered that are present in the molecule;  $x$  of them are located at the reactive site;  $z$  of which are in intramolecular isotopic competition. <sup>c</sup> Correctly evaluated analogous to eqs 14/15. <sup>d</sup> Approximated by  $\epsilon_{\text{reactive position}} \approx n/x \cdot \epsilon_{\text{bulk}}$  (eq 16). <sup>e</sup> Italic numbers indicate values outside the typical range.

to about 50% bond cleavage based on the Streitwieser Limit for a C–Cl bond (see Table 1). With iron sulfides lower AKIE<sub>C</sub> values of 1.016 were found, indicating either the presence of a slow, nonfractionating step such as formation of substrate–surface complexes or an unusually low extent of C–Cl bond cleavage in the transition state at the FeS surface (81).

Several studies investigated isotope fractionation during hydrogenolysis of chlorinated ethenes. Although the anaerobic microbial dechlorination of these compounds is still not understood in detail, insight exists from mechanistic studies with cobalamin (vitamin B12) as an abiotic model system (82–84). Evidence from these studies indicates that the initial step in tetrachloroethene (PCE) and, possibly, also TCE degradation is a dissociative single-electron transfer in which one C–Cl bond is cleaved and a radical is formed. In terms of isotope fractionation this means that only one carbon center is involved. Values of  $\epsilon_{\text{bulk}}$  reported by Slater et al. (85) may therefore be corrected for intramolecular competition (PCE:  $n=2$ ,  $x=2$ ,  $z=2$ ) and nonreacting locations (TCE:  $n=2$ ,  $x=1$ ,  $z=1$ ), leading to AKIE<sub>C</sub> values of 1.033–1.036, which are only slightly larger than those in transformation of CCl<sub>4</sub> with nonsulfidic iron(II) bearing minerals (see Table 8). If one assumes that transformation of PCE and TCE in biotic systems occurs by a similar mechanism as for cobalamin, then the reported  $\epsilon_{\text{bulk}}$  values (PCE: –2‰ to –5‰, TCE: –2.5‰ to –13.8‰) would lead to AKIE<sub>C</sub> values of 1.004–1.010 (PCE) and 1.005–1.028 (TCE), which are for the most part substantially smaller than those measured by Slater et al. for vitamin B12. Again this may indicate the presence of commitment to catalysis and/or other rate-limiting steps. In contrast to the reaction of vitamin B12 with PCE and TCE, evidence by Glod et al. (83) indicates that the initial step with *cis*-/*trans*-dichloroethene (*cis*-/*trans*-DCE) and VC is probably concerted. They postulated a nucleophilic addition of cob(I)alamin to one of the carbon atoms of the ethene and simultaneous protonation of the other carbon atom. Hence,  $\epsilon_{\text{bulk}}$  values have to be converted into AKIE<sub>C</sub> per carbon atom *without* further correction. The reported values for *cis*-DCE (–14.1‰ (86) to –25.5‰ (87) and VC (–21.5‰ (86) to –31.1‰ (88) support this hypothesis. For example, taking the value for VC of –31.1‰, if one assumes that the reaction was *not* concerted and initially only one C–Cl bond was broken, a correction would have to be made for the nonreacting location ( $n=2$ ,  $x=1$ ). According to eq 22, an AKIE<sub>C</sub> of 1.066 would then be obtained. As this value seems unrealistically high for cleavage of a C–Cl bond, one can

conclude that the reaction under investigation was probably concerted, in agreement with the mechanistic model of Glod et al. (83).

In the case of chlorinated ethene reduction by zerovalent metals similar effects can be expected to be at work. For the reaction at a precleaned iron surface, Arnold and Roberts (89) have postulated a di- $\sigma$ -bonded surface-bound intermediate meaning that the reaction would involve both carbon centers of the ethene. However, in zerovalent iron subsurface barriers, where iron oxide layers may form at the barrier surface, the initial step could possibly also be a dissociative single-electron transfer, in which case only one carbon center would be involved. In addition, fractionation can be expected to depend critically on the rate of the surface reaction relative to other possible rate determining steps such as transport and sorption to reactive sites. All of these parameters (type of intrinsic reaction, number of carbon centers involved, commitment to catalysis) can be expected to depend critically on the properties and corrosion state of the manufactured iron. It is, therefore, not surprising that reported  $\epsilon_{\text{bulk}}$  values for this reaction have been found to vary considerably (PCE: –5.7‰ to –25.3‰ (90, 91); TCE: –7.5‰ to –24.8‰ (90–93); *cis*-DCE: –6.9‰ to –16.0‰ (90, 91); VC: –6.9‰ to –19.3‰ (90)). Evidence for a subtle influence of iron pretreatment on observed  $\epsilon_{\text{bulk}}$  values is also given by a recent study of Slater et al. (92). Further insight can possibly be obtained in detailed future studies that address isotope fractionation of multiple elements and may be complemented by a time-dependent surface analysis of the zerovalent metal barrier.

For dichloroelimination of chlorinated alkanes, finally, it is also not clear if the rate limiting step involves only one or both carbons. Although overall two C–Cl bonds are broken in the reductive dichloroelimination of chlorinated alkanes, Roberts et al. (48) and Arnold et al. (49) have argued that the reaction is not necessarily concerted. Often the initial step may be the cleavage of only one of the two C–Cl bonds leading to radical intermediates (49). Consequently, without detailed knowledge about the stepwise or concerted character of the reaction, it is difficult to interpret observed  $\epsilon_{\text{bulk}}$  in terms of apparent kinetic isotope effects. However, for similar reasons as discussed above, the very large  $\epsilon_{\text{bulk}}$  of –32‰ reported by Hunkeler et al. (2002) in the reductive dechloroelimination of 1,2-dichloroethane (88) would not be consistent with a stepwise mechanism so that for this

**TABLE 9. Assuming Different Reaction Scenarios for Anaerobic MTBE Degradation, AKIE Values Are Derived from Experimental Data and Compared to Typical KIE Ranges for Each of the Reactions<sup>d</sup>**

mechanistic scenario	element	reported $\epsilon_{\text{bulk}}$	ref	$n^a$	$x^a$	$\epsilon_{\text{reactive position}}$	$z^b$	$Z \cdot \epsilon_{\text{reactive position}}$	AKIE obtained	KIE expected	$\frac{[\alpha_{\text{rp,H}}]^{-1} - 1}{[\alpha_{\text{rp,C}}]^{-1} - 1}$		scenario consistent
											obtained	expected	
<b>Anaerobic Biodegradation</b>													
methyl group oxidation	C	-9.2‰ to -15.6‰ <sup>b</sup>	carbon: (105, 9, 132)	5	1	-46.0 to -78.0‰	1	-46.0 to -78.0‰	1.048 to 1.085	1.01 to 1.03	0.5 to 1.9	7 to 48	no
	H	-11‰ to -21‰ <sup>c</sup>		12	3	-44‰ to -84‰	3	-132‰ to -252‰	1.15 to 1.33	2 to 50			
S <sub>N</sub> 1	C	-9.2‰ to -15.6‰ <sup>b</sup>	hydrogen: (94)	5	1	-46.0 to -78.0‰	1	-46.0 to -78.0‰	1.048 to 1.085	1.00 to 1.03	0.2 to 0.6	1.6 to 8 (for KIE <sub>C</sub> = 0)	no
	H	-11‰ to -21‰ <sup>c</sup>		12	9	-15‰ to -28‰	1	-15‰ to -28‰	1.02 to 1.03	1.05 to 1.15			
S <sub>N</sub> 2	C	-9.2‰ to -15.6‰ <sup>b</sup>		5	1	-46.0 to -78.0‰	1	-46.0 to -78.0‰	1.048 to 1.085	1.03 to 1.09	0.5 to 1.9	-0.6 to 1.7	yes
	H	-11‰ to -21‰ <sup>c</sup>		12	3	-44‰ to -84‰	1	-44‰ to -84‰	1.05 to 1.09	0.95 to 1.05			
<b>Aerobic Biodegradation</b>													
methyl group oxidation	C	-1.5‰ to -2.4‰	carbon: (65, 64)	5	1	-7.3‰ to -11.0‰	1	-7.3‰ to -11.0‰	1.007 to 1.011	1.01 to 1.03	14 to 34	7 to 48	yes
	H	-29‰ to -66‰	hydrogen: (65)	12	3	-136‰ to -202‰	3	-408‰ to -606‰	1.69 to 2.54	2 to 50			

<sup>a</sup>  $n$ : number of atoms of the element considered that are present in the molecule;  $x$  of them are located at the reactive site;  $z$  of which are in intramolecular isotopic competition. <sup>b</sup> The range reflects variations in  $\epsilon_{\text{bulk}}$  and includes also to the most part the rather large 95% confidence intervals of these studies. <sup>c</sup> Range given as 95% confidence intervals as reported in the study by Kuder et al. (94). <sup>d</sup> In addition, also the *ratios* of observed and expected hydrogen and carbon isotope fractionation are given, expressed in the form  $[(\alpha_{\text{rp,H}})^{-1} - 1]/[(\alpha_{\text{rp,C}})^{-1} - 1]$ . For comparison, the calculation is also carried out for aerobic MTBE degradation, where the degradation mechanism is known.

particular case a concerted character of the reaction may be inferred.

In conclusion, the comparison of AKIE values for different molecules undergoing the same reaction demonstrates that in most cases observed values are well in the range expected from theoretical considerations. However, if non- or little fractionating slow steps precede the actual transformation, the observed AKIE may occasionally be considerably smaller. Therefore, if one attempts to use isotope effects to *identify* reactions, it is important to bear in mind that the evidence is strongest if the value is *above* a certain threshold value typical for the reaction. Examples are high carbon KIE for an S<sub>N</sub>2 reaction or reductive C–Cl bond cleavage and large hydrogen KIE for oxidation of an alkyl-group. Care must finally be taken to recognize cases where a reaction may be concerted, as otherwise erroneous AKIE values may be calculated.

### Elucidation of Reaction Pathways: Testing Different Degradation Scenarios Based on AKIE Values

So far we have shown that calculations of AKIE are very helpful in establishing common isotope fractionation patterns for cases of well-known degradation reactions. However, such an evaluation may even be more powerful when applied to degradation processes in which the transformation pathway is yet uncertain, particularly if isotope fractionation of two different elements (e.g., H, C) is available. An example is the *anaerobic* transformation of methyl *tert*-butyl ether (MTBE) of which the reaction pathway has not yet been clearly identified. In principle, initial transformation of MTBE may occur by (see Scheme 1) (1) oxidation of the methyl group (such as in the *aerobic* transformation, see above), (2) acid-catalyzed hydrolysis involving the *tert*-butyl-group (S<sub>N</sub>1 reaction), or (3) hydrolysis by nucleophilic attack at the methyl group (S<sub>N</sub>2 reaction).

Although all three paths finally lead to the common product *tert*-butyl alcohol (TBA), they can be expected to be

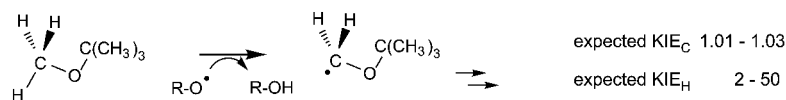
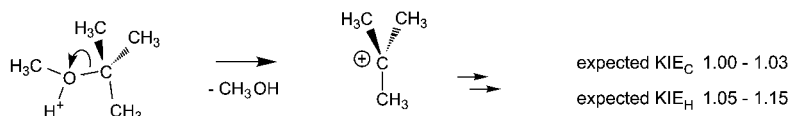
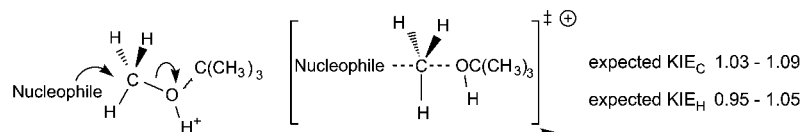
very different with respect to isotope fractionation. Not only are different bonds cleaved but also the reaction involves entirely different parts of the MTBE molecule. Consequently, each case requires a separate evaluation. For carbon isotopes, the correction is straightforward. In all three cases, the reactions takes place at one of the five carbon atoms and thus  $n = 5$  and  $x = 1$ .

For hydrogen isotopes, reaction (1) involves breaking of a C–H bond of the methyl group, and thus a primary hydrogen KIE is expected. Given that MTBE has 12 H atoms and that intramolecular competition occurs between the three H atoms in the methyl group,  $n = 12$ ,  $x = 3$ , and  $z = 3$ . In reactions (2) and (3), a C–O bond is broken, and thus only a secondary hydrogen KIE occurs. In the absence of a large primary effect, secondary isotope effects must be addressed in a special way. For one thing they can then not be neglected, and for another, there will generally be no intramolecular competition. In acid hydrolysis of MTBE (S<sub>N</sub>1 reaction), for example, no C–H bond is actually broken so that no primary hydrogen isotope effect can be expected. Instead, the nine hydrogen atoms in the *tert*-butyl group (CH<sub>3</sub>–O–C(CH<sub>3</sub>)<sub>3</sub>) are instrumental in stabilizing the positive charge at the carbon atom in the transition state when the cation [C<sup>+</sup>(CH<sub>3</sub>)<sub>3</sub>] is formed (hyperconjugation). Therefore, if any one of them is deuterium, it will slightly affect the rate of [C<sup>+</sup>(CH<sub>2</sub>D)(CH<sub>3</sub>)<sub>2</sub>] formation, thus causing a secondary isotope effect. However, because hyperconjugation is such a “concerted action” of all nine positions, there will be no intramolecular competition between them. Thus for S<sub>N</sub>1, the following parameters for calculation of the AKIE have to be used:  $n = 12$ ,  $x = 9$ , and  $z = 1$ . Finally, for the S<sub>N</sub>2 reaction, only the 3 H-atoms bound to the methyl group can cause a secondary KIE, and, similar as for S<sub>N</sub>1, no intramolecular competition occurs. Hence for S<sub>N</sub>2, the parameters are  $n = 12$ ,  $x = 3$ , and  $z = 1$ .

The results of the AKIE calculations for the different scenarios are summarized in Table 9 and compared to typical KIE ranges. The high carbon AKIE<sub>C</sub> of 1.042–1.085 that is

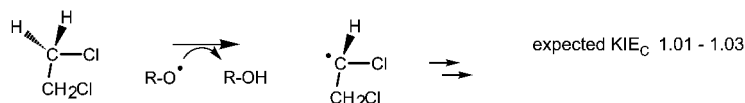
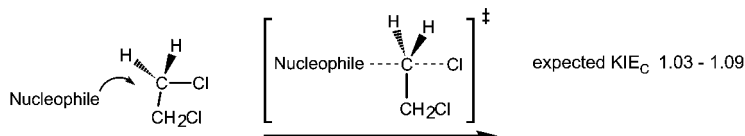
## SCHEME 1

(1) oxidation of a C-H bond in the methyl group of MTBE

(2) acidic hydrolysis of MTBE ( $S_N1$ -reaction)(3) hydrolysis of MTBE by (enzymatic) nucleophilic attack ( $S_N2$ -reaction)

## SCHEME 2

(1) oxidation of a C-H bond in 1,2-dichloroethane

(2) hydrolysis of 1,2-dichloroethane by (enzymatic) nucleophilic attack ( $S_N2$ -reaction)

obtained for all scenarios is only consistent with an  $S_N2$ -like nucleophilic substitution, possibly by a hydrolase enzyme in a microbial degradation reaction. Also the hydrogen  $AKIE_H$  of 1.05–1.07 calculated for this scenario falls just in the upper range of the region that is expected for an  $S_N2$ -reaction. In contrast, oxidation or hydrolysis via an  $S_N1$ -like hydrolysis can be ruled out as possible pathways, because calculated  $AKIE$  are not consistent with the  $KIE$  expected for these scenarios. To our knowledge, this is the first mechanistic evidence that has been provided on anaerobic biodegradation of MTBE (71, 94). The large  $AKIE_C$  for  $S_N2$  also demonstrates that commitment to catalysis was probably small. For comparison, the values for the known *aerobic* reaction are also given in Table 9. The substantial hydrogen  $AKIE_H$  is consistent with the mechanistic model that MTBE is transformed by initial methyl-group oxidation. Both the carbon and hydrogen  $AKIE$  are close to the lower range of values expected for this reaction, possibly due to some reduction of the  $AKIE$  by elevated commitment to catalysis.

Another example illustrating the usefulness of  $AKIE$  values for the identification of degradation pathways is a recent laboratory study on aerobic biodegradation of 1,2-dichloroethane by Hirschorn et al. (95). Under seemingly identical conditions in laboratory experiments, carbon isotope fractionation was found to vary greatly and in a bimodal fashion, not only between experiments with enrichment cultures from different field sites but also in the same enrichment culture over time. Calculation of  $AKIE_C$  values gave numbers of 1.01 and 1.06, typical of oxidation and  $S_N2$  hydrolysis, respectively

so that the cause of the variations could be attributed to different degradation pathways (see Scheme 2).

## Dealing with Commitment to Catalysis

As already mentioned above, nonfractionating slow steps can occasionally complicate an identification of degradation pathways, as calculated  $AKIE$  values may then be no longer characteristic of a certain reaction. As discussed in the Supporting Information, this phenomenon will be especially strong if elevated commitment to catalysis and intramolecular isotopic competition occur simultaneously, particularly in the case of large hydrogen isotope effects. (One would actually first have to take into account the influence of masking and then correct for intramolecular competition, see the detailed discussion in the Supporting Information.) Unfortunately, there is no straightforward approach to estimate the extent of commitment to catalysis using compounds that are composed of isotopes at natural abundance. An analysis in terms of transformation pathways may nonetheless be possible, if isotope signatures are measured for *two elements simultaneously*. The reason is that the effect of commitment to catalysis acts on both elements at the same time so that their isotope data may be considered *relative to each other*. Such a comparison is straightforward if eq 23 is applied. (In the Supporting Information it is shown how the derivation of this formula elegantly eliminates contributions from commitment to catalysis.)

$$\frac{(\alpha_{\text{tp,H}})^{-1} - 1}{(\alpha_{\text{tp,C}})^{-1} - 1} = \frac{\text{KIE}_\text{H} - 1}{\text{KIE}_\text{C} - 1} \cdot \frac{1 + \text{KIE}_\text{C} \cdot (z_\text{C} - 1)}{1 + \text{KIE}_\text{H} \cdot (z_\text{H} - 1)} \quad (23)$$

Here,  $\alpha_{\text{tp,H}}$  and  $\alpha_{\text{tp,C}}$  are the hydrogen and carbon fractionation factors at the reacting position that are obtained from experimental data after correction for nonreacting locations (eqs 14/15).  $\text{KIE}_\text{H}$  and  $\text{KIE}_\text{C}$  are the expected kinetic isotope effects, and the term including the factors  $z_\text{C}$  and  $z_\text{H}$  is in this case the appropriate correction for intramolecular competition. For a given reaction, the term on the right-hand-side of the equation can be calculated based on the expected KIEs for different elements, and it can then be compared to the experimentally determined ratio on the left-hand side. Note that in cases where  $\alpha_{\text{tp}}$  is close to unity and  $\epsilon_{\text{rp}}$  is very small, the ratio of  $[(\alpha_{\text{tp,H}})^{-1} - 1]/[(\alpha_{\text{tp,C}})^{-1} - 1]$  is approximately equivalent to the ratio  $\epsilon_{\text{rp,H}}/\epsilon_{\text{rp,C}} = [\alpha_{\text{tp,H}} - 1]/[\alpha_{\text{tp,C}} - 1]$ . The approximation is generally valid with  $\epsilon_{\text{rp,C}}$ , whereas with  $\epsilon_{\text{rp,H}}$  it is frequently not. Hence, *qualitative* differences in fractionation patterns can already be derived from comparing  $\epsilon_{\text{rp,H}}/\epsilon_{\text{rp,C}}$  ratios or from simply plotting measured  $\delta^{2}\text{H}$  vs  $\delta^{13}\text{C}$  signatures, which yield a relationship with a slope corresponding approximately to  $\epsilon_{\text{bulk,H}}/\epsilon_{\text{bulk,C}}$ . Such a two-dimensional isotope plot is sketched at the right-hand side of Figure 2 and can be found in Zwank et al. Figure 6 (71), Kuder et al. Figure 2 (94), or Hunkeler et al. Figure 2 (96). The main advantages of such plots is that they are intuitively accessible and can be constructed even from field data, as the necessity is eliminated to determine the precise fraction of remaining substrate  $f$ , which would be needed to calculate  $\epsilon_{\text{reactive position}}$  values (see below). In laboratory experiments, however, where data on  $f$  are available, we recommend using in the well-understood eq 23, which makes it possible to test mechanistic scenarios actually in comparison with published AKIE values. This is again illustrated for the example of MTBE. The obtained and expected values corresponding to the terms on the left- and right-hand side of eq 23 are given in Table 9. For anaerobic MTBE degradation, the values are at least an order of magnitude apart in the case of oxidation of the methyl group and the  $\text{S}_\text{N}1$  reaction, while good agreement is again observed for the  $\text{S}_\text{N}2$  reaction indicating that this reaction is occurring. Similarly, expected and observed values match well for aerobic MTBE oxidation.

### Consequences for the Assessment of Isotope Fractionation in the Field

The ultimate goal in field applications of CSIA is usually to *quantify* the extent of contaminant transformation. The general feasibility of such an approach has been demonstrated in a number of studies (71, 97–103) and is discussed in a comprehensive recent review by Meckenstock et al. (24). Here we focus primarily on the aspect how insight about transformation pathways can aid in choosing the appropriate isotopic enrichment factor ( $\epsilon_{\text{bulk}}$ ) that is needed to quantify the extent of in situ transformation according to eq 8. In cases of compounds that undergo only one type of transformation (e.g., degradation of toluene under anaerobic conditions) only the variability in  $\epsilon_{\text{bulk}}$  for the same type of reaction (i.e., cleavage of a C–H bond) must be considered to assess how reliable the result is (66). However, as we have shown above, a more substantial and systematic variation of isotopic enrichment factors can be observed if a given pollutant is transformed by *different* mechanisms (see for example MTBE or 1,2-DCA (71, 94, 95)). Clearly, in such cases, the in situ identification of the reaction mechanism in the field is crucial for the choice of reliable  $\epsilon_{\text{bulk}}$  values. One possibility to identify a reaction mechanism is to estimate  $\epsilon_{\text{bulk}}$  from field isotope and concentration data and compare it to values for known reaction mechanisms possibly after conversion to AKIE. At field sites with wide plumes where

transversal dispersion does not strongly affect concentrations along the plume centerline, concentrations and isotope ratios have indeed occasionally been found to be correlated, and regressions according to the Rayleigh equation agreed with  $\epsilon_{\text{bulk}}$  values previously determined in laboratory experiments (99, 101, 104). Since in other cases concentration data can be much more strongly affected by dilution, the obtained isotopic enrichment factors are often smaller than laboratory values, such as for example observed for MTBE contaminated aquifers (71, 94, 105). An alternative approach to identify a reaction mechanism is, therefore, the evaluation of isotope data of multiple elements that are fractionated at different proportions by the different mechanisms. As shown by Zwank et al. (71) and Kuder et al. (94) for the case of MTBE, a plot of measured carbon vs hydrogen isotope ratios such as sketched in the box at the right side of Figure 2 (“two-dimensional isotope analysis”) bears the same characteristic information as eq 23 and may therefore be used to identify degradation pathways even under such complex conditions. This approach is not only insensitive to the effect of masking (see discussion above) but also to the influence of dilution because both elements will be affected in the same way.

Finally, an additional source of uncertainty must be taken into account, even if isotopic enrichment factors ( $\epsilon_{\text{bulk}}$ ) values are known from laboratory experiments, if the transformation mechanism has been identified using the two-dimensional approach and if the degree of pollutant transformation is quantified using the Rayleigh law in form of eq 8. When discussing the precision of such an approach in the field, it must be considered that uncertainty is not only introduced by variability of the isotopic enrichment factors but also because the assumption of a homogeneous contaminant pool underlying the Rayleigh equation is not necessarily fulfilled in heterogeneous systems such as groundwater flow. Contaminants will travel along different paths and reach a monitoring point after different travel times, a phenomenon that is usually lumped into a dispersion parameter. Accordingly, a groundwater sample will consist of a mixture of molecules having experienced a different degree of degradation and isotope fractionation. This phenomenon is expected to lead to a smaller shift in isotope ratios than expected for a homogeneous compound pool and thus to an underestimation of transformation if evaluated using the Rayleigh equation.

### Implications and Future Research Needs

The main goal of the review was to provide more insight into the factors that control the magnitude of isotope fractionation of organic molecules by relating the observed isotope fractionation to reaction mechanisms. As discussed above, a number of factors could be identified that influence observable isotope fractionation: (1) The number of total ( $n$ ), nonreacting ( $n-x$ ), and intramolecular competing ( $z$ ) positions of an element inside an organic compound. (2) Different degradation reactions involving different bonds within a molecule which lead to different characteristic kinetic isotope effects. (3) The extent of bond changes in the transition state that introduces variability even for the same degradation reaction. (4) The masking of the intrinsic isotope effect by slow preceding steps, which can be described in terms of commitment to catalysis.

As shown in this review, it is in many cases possible to address the first two aspects and to uncover apparent kinetic isotope effects that are both position-specific and characteristic of the degradation reaction. Using the novel approach presented, much of the uncertainty can be removed, and mechanistic insight may be used to back up the appropriate choice of  $\epsilon_{\text{bulk}}$  for quantification of in situ degradation in the field (see discussion above and Figure 2). According to the approximate eq 22, which expresses the mutual interde-



pendence of AKIE and  $\epsilon_{\text{bulk}}$  values, one can even *predict* the approximate magnitude of isotope fractionation for new compounds and, thus, decide whether isotope studies of hitherto not investigated contaminants are feasible. The approximate estimate of  $\epsilon_{\text{bulk}}$  values, as it was recently performed for anaerobic degradation of toluene, xylenes, and related compounds (66), is therefore now possible with degradation scenarios of any chosen contaminant, provided that KIE values of the respective transformation reactions are already published.

However, considerable variability is still introduced by the latter two aspects, that is, transition state structure and masking: The variability introduced by the transition state structure is reflected in the spread of the typical KIE values given in Table 2, whereas AKIE values that are listed in Tables 3–9 are in addition also subject to the influence of masking. As is evident from the interdependence of AKIE and  $\epsilon_{\text{bulk}}$  values derived in this review (e.g., as expressed by the approximate eq 22), these variations will be directly reflected in the corresponding  $\epsilon_{\text{bulk}}$  values. This raises the question how or whether the variability associated with factors 3 and 4 can be further addressed in the future.

Regarding the effect of bond changes in the transition state, it has to be noted that the reference values summarize KIEs for a given reaction mechanism acting on different molecules. Therefore, some variation has to be expected for the same type of transformation, no matter whether it occurs with different compounds in the same microorganism or if it happens with the same compound in different microorganisms. An approach to further constrain this variability is to calculate reference values for a specific reaction acting on a specific molecule. This approach is only feasible if the structure of the transition state is sufficiently known, as was shown recently for chlorine isotope effects associated with dehalogenation of chlorinated alkanes by a haloalkane dehalogenase (106). A good agreement between calculated and experimental values was observed. While it may not be feasible to derive reference values for each reaction and each compound, there is clearly a need for more reference values for various types of environmentally relevant reactions, either of experimental origin or calculated. For example, in addition to the reactions mentioned earlier in this review, KIE data are also reported for  $\beta$ -elimination reactions (H and leaving group isotopes: ref 107, chapter 4, refs 108 and 109), acid and base-catalyzed hydrolysis at the carboxyl group of esters and amides (C, O and H isotopes: refs 37 and 110), abiotic (111–113) and biotic (110, 114) hydrolysis of phosphoesters, phosphorothioesters (115), or even sulfate esters (116) (O-isotopes). Conversely, in the case of redox reactions, degradation by direct photolysis or reactions of less frequently analyzed elements such as N or O data are often still missing. Studies in contaminant hydrology can play a pioneering role by generating such crucial reference information that may be of great relevance also for other disciplines.

Regarding commitment to catalysis, its effect could be quantified if the elemental rate constants for the different steps involved in enzymatic transformation are known. However, these rates are difficult to determine and are only known in exceptional cases (17). Presently we are only at the beginning of such a detailed understanding of biotransformations in living organisms. However, isotope studies can play a key role in their elucidation in the future owing to the unique insight that they can provide into commitment to catalysis (17). They represent an important tool that is complementary to existing microbiological methods.

The uncertainty associated with factors 3 and 4 has also implications when the evaluation procedure is used to *predict* the isotope fractionation factor for a compound that is transformed by a known pathway according to eq 22. As the actual fractionation factor may be smaller due to elevated

commitment to catalysis, such estimated values cannot be directly used to quantify pollutant degradation. Despite our now much more advanced understanding, controlled laboratory studies with specific compounds will therefore still be needed in the future in order to confine the ranges of possible  $\epsilon_{\text{bulk}}$  values and determine ranges that may be used to calculate conservative estimates of quantification in the field.

Finally, in addition to the factors summarized above and discussed in detail in this paper, there are additional factors that affect the magnitude of isotope fractionation and interpretation of isotope data and thus need further attention in the future. Among them are the effect of temperature, the observation of non-Rayleigh type behavior and the effect of uneven intramolecular isotope distribution. From chemical studies it is well established (117–119, 120–124) that temperature can have an influence on observable isotope effects so that values observed in laboratory studies (293–298 K) may deviate from those in the wide range of temperatures encountered in the environment (277–313 K). Considering transformation reactions of contaminants, this important aspect has been investigated only for the degradation of toluene by different microorganisms (76) where temperature effects were found to be negligible. It remains to be seen whether this result is typical also of other degradation reactions or whether it is primarily attributable to the anomalously weak temperature dependence that is known to exist for the microbial cleavage of C–H bonds (125).

The evaluation procedure developed in this paper relies on the assumption that the KIE remains constant during degradation of a compound. While constant fractionation factors obtained in many studies support this assumption, there are cases where a non-Rayleigh type of isotope evolution was observed. Such a behavior can be due to two main reasons that deserve further attention: (1) In case of enzymatic reactions, the commitment to catalysis may vary due to changes in environmental conditions (e.g. pH) or changes in cosubstrate concentration. (2) The degradation may include parallel pathways whose proportion changes as contaminant degradation proceeds, e.g., due to differences in affinity of the different enzymes.

Finally, one aspect that has largely been overlooked so far is the effect of the intramolecular isotope distribution inside contaminants. Depending on whether the “label” in the form of heavy isotopes is enriched in the reacting or nonreacting locations of an organic compound, observable isotope fractionation may be unusually strong or non-existent, *despite the same intrinsic (A)KIE value at the reactive site!* As mentioned earlier in this article, according to current practice (i.e., comparisons of  $\epsilon_{\text{bulk}}$  values from different laboratories) it is, therefore, silently assumed that isotopes are distributed evenly inside a molecule. In the Supporting Information, part 5 we discuss in detail why this assumption is a good approximation in the case of carbon and, likely, also often for hydrogen isotopes. Particularly in the case of hydrogen, however, it is strongly recommended to actually determine the intramolecular isotope distributions by SNIF-NMR analysis (Site-Specific Natural Isotope Fractionation by Nuclear Magnetic Resonance Spectroscopy) before conducting degradation experiments that are analyzed by GC–IRMS in future laboratory studies.

## Abbreviations

AKIE, AKIE<sub>E</sub> position-specific *apparent* kinetic isotope effect of element E evaluated according to eq 21; for differences between AKIE and KIE see eq 3 and Supporting Information

$\alpha$ , $\alpha_{\text{bulk}}$	fractionation factor evaluated according to the “traditional” Rayleigh equation (eq 6,7); see also eq 4	R	ratio of molecules containing a heavy isotope to molecules containing only light isotopes; for difference to $R$ see Supporting Information
$\alpha_{\text{reactive position}}$ , $\alpha_{\text{rp,E}}$	fractionation factor of element E at the reacting position evaluated after correction for nonreacting positions (eq 14/15); see also eqs 10/11	$S_{\text{N}1}$ , $S_{\text{N}2}$	first- and second-order nucleophilic substitution reactions
B	extent of in situ biodegradation calculated according to eq 8	SNIF-NMR	Site-Specific Natural Isotope Fractionation by Nuclear Magnetic Resonance Spectroscopy
C	commitment to catalysis, given by a mathematical expression that can be written in terms of rate constants of enzyme catalysis (eq 3)	TBA	<i>tert</i> -butyl alcohol
CSIA	Compound Specific Isotope Analysis	TCE	trichloroethene
<i>cis</i> -DCE	<i>cis</i> -dichloroethene	VC	vinyl chloride
1,2-DCA	1,2-dichloroethane	$x$	number of atoms of element E that are located in reactive positions (see eqs 12/13)
$\delta^{\text{h}}\text{E}$ (e.g., $\delta^{13}\text{C}$ )	isotope signature: bulk abundance of heavy isotopes (= average over all positions of an organic compound), expressed as difference in permil with respect to an international reference standard (eq 1); $\delta^{\text{h}}\text{E}_0$ : value at beginning of reaction	$z$ , $z_{\text{E}}$	number of atoms of element E in indistinguishable, reactive positions between which intramolecular isotopic competition exists (see eq 21)
$\Delta\delta^{\text{h}}\text{E}$ (e.g., $\Delta\delta^{13}\text{C}$ )	(= $\delta^{\text{h}}\text{E} - \delta^{\text{h}}\text{E}_0$ ) difference between the bulk isotope signature at time $t$ and the beginning of a reaction		
$^{\text{h}}\text{E}$ , $^{\text{l}}\text{E}$	heavy and light isotopes of element E (e.g., E = H, C, N, O, S, Cl)		
$\epsilon$ , $\epsilon_{\text{bulk}}$	enrichment factor evaluated according to the “traditional” Rayleigh equation (eqs 6/7)		
$\epsilon_{\text{reactive position}}$ , $\epsilon_{\text{rp,E}}$	enrichment factor of element E at the reacting position evaluated after correction for nonreacting positions (eqs 14/15)		
$\epsilon_{\text{intrinsic}}$	term introduced by Morasch et al. <sup>66</sup> as an operational correction for the number of atoms of E inside a compound (see eq 22)		
$f$	fraction of substrate remaining ( $C/C_0$ )		
GC–IRMS	Gas Chromatography – Isotope Ratio Mass Spectrometry		
$i$	$i$ order of kinetic rate law (e.g., $i = 2$ with a second-order reaction, eq 9)		
KIE, $\text{KIE}_{\text{E}}$	position-specific kinetic isotope effect of element E defined as $^{\text{l}}k/^{\text{h}}k$ (eq 2)		
$^{\text{h}}k$ , $^{\text{l}}k$	rate constants of bonds containing a heavy/light isotopes of element E, e.g., $^2k$ , $^{\text{l}}k$ (H), $^{13}k$ , $^{12}k$ (C), etc.		
MTBE	methyl <i>tert</i> -butyl ether		
$n$	number of atoms of element E inside an organic compound		
PCE	tetrachloroethene		
$R$	$R = ^{\text{h}}\text{E}/^{\text{l}}\text{E}$ , “bulk“ ratio of heavy ( $^{\text{h}}\text{E}$ ) and light ( $^{\text{l}}\text{E}$ ) isotopes of a given element E, as average over all molecular positions of a given compound; $R_0$ : value at beginning of reaction (eq 1)		

## Acknowledgments

We thank Barbara Sherwood Lollar, Stefan Haderlein, Michael Berg, Torsten Schmidt, Rainer Meckenstock, Ramon Aravena, Thomas Hofstetter, Andreas Kappler, Christoph Aeppli, Akané Hartenbach, and four anonymous reviewers for very helpful comments on the manuscript. Thanks to Georges Lacrampe-Couloume, Uli Wortmann, Carsten Schubert, Penny Morill, Nancy VanStone, Jennifer McKelvie (Gray), Silvia Mancini, Sarah Hirschorn, and Michelle Chartrand for stimulating discussions. Jennifer McKelvie (Gray) provided the original data on aerobic MTBE degradation that allowed the reevaluation given in Tables 3 and 4. This work was supported by the German Research Foundation (DFG) through the Research Fellowship EL 266/1 of M.E.

## Supporting Information Available

Experimental determination of isotope ratios; background information related to the rules of thumb; kinetic isotope effects reported in the literature (continued); mathematical derivation of the novel evaluation procedure; mathematical derivation of the approximate eqs 16 and 22 and illustration of associated errors; influence of a nonstatistical isotope distribution inside organic compounds; and reevaluation of original data on aerobic MTBE degradation of Hunkeler et al. This material is available free of charge via the Internet at <http://pubs.acs.org>.

## Literature Cited

- (1) Clark, I.; Fritz, P. *Environmental isotopes in hydrogeology*; Lewis Publishers: New York, 1997; p 328.
- (2) Hoefs, J. *Stable isotope geochemistry*; Springer-Verlag: Berlin, 1997.
- (3) Brenna, J. T.; Corso, T. N.; Tobias, H. J.; Caimi, R. J. High-precision continuous-flow isotope ratio mass spectrometry. *Mass Spectrom. Rev.* **1997**, *16*, 227–258.
- (4) Meier-Augenstein, W. Applied gas chromatography coupled to isotope ratio mass spectrometry. *J. Chromatogr. A* **1999**, *842*, 351–371.
- (5) Matthews, D. E.; Hayes, J. M. Isotope-ratio-monitoring gas chromatography–mass spectrometry. *Anal. Chem.* **1978**, *50*, 1465–1473.
- (6) Merritt, D. A.; Freeman, K. H.; Ricci, M. P.; Studley, S. A.; Hayes, J. M. Performance and optimization of a combustion interface for isotope ratio monitoring gas-chromatography mass-spectrometry. *Anal. Chem.* **1995**, *67*, 2461–2473.

- (7) Burgoyne, T. W.; Hayes, J. M. Quantitative production of H-2 by pyrolysis of gas chromatographic effluents. *Anal. Chem.* **1998**, *70*, 5136–5141.
- (8) Dempster, H. S.; Sherwood Lollar, B.; Feenstra, S. Tracing organic contaminants in groundwater: A new methodology using compound specific isotopic analysis. *Environ. Sci. Technol.* **1997**, *31*, 3193–3197.
- (9) Slater, G. F.; Dempster, H. S.; Sherwood Lollar, B.; Ahad, J. Headspace analysis: A new application for isotopic characterization of dissolved organic contaminants. *Environ. Sci. Technol.* **1999**, *33*, 190–194.
- (10) Hunkeler, D.; Aravena, R. Determination of stable carbon isotope ratios of chlorinated methanes, ethanes and ethenes in aqueous samples. *Environ. Sci. Technol.* **2000**, *34*, 2839–2844.
- (11) Zwank, L.; Berg, M.; Schmidt, T. C.; Haderlein, S. B. Compound-specific carbon isotope analysis of volatile organic compounds in the low-microgram per liter range. *Anal. Chem.* **2003**, *75*, 5575–5583.
- (12) Schmidt, T. C.; Zwank, L.; Elsner, M.; Berg, M.; Meckenstock, R. U.; Haderlein, S. B. Compound-specific stable isotope analysis of organic contaminants in natural environments: A critical review of the state of the art, prospects, and future challenges. *Anal. Bioanal. Chem.* **2004**, *378*, 283–300.
- (13) Sherwood Lollar, B.; Slater, G. F.; Ahad, J.; Sleep, B.; Spivack, J.; Brennan, M.; MacKenzie, P. Contrasting carbon isotope fractionation during biodegradation of trichloroethylene and toluene: Implications for intrinsic bioremediation. *Org. Geochem.* **1999**, *30*, 813–820.
- (14) Heraty, L. J.; Fuller, M. E.; Huang, L.; Abrajano, T.; Sturchio, N. C. Isotope fractionation of carbon and chlorine by microbial degradation of dichloromethane. *Org. Geochem.* **1999**, *30*, 793–799.
- (15) Meckenstock, R. U.; Morasch, B.; Warthmann, R.; Schink, B.; Annweiler, E.; Michaelis, W.; Richnow, H. H.  $^{13}\text{C}/^{12}\text{C}$  isotope fractionation of aromatic hydrocarbons during microbial degradation. *Environ. Microbiol.* **1999**, *1*, 409–414.
- (16) Hunkeler, D.; Aravena, R.; Butler, B. J. Monitoring microbial dechlorination of tetrachloroethene (PCE) using compound-specific carbon isotope ratios: Microcosms and field experiments. *Environ. Sci. Technol.* **1999**, *33*, 2733–2738.
- (17) Hunkeler, D.; Aravena, R. Evidence of substantial carbon isotope fractionation between substrate, inorganic carbon, and biomass during aerobic mineralization of 1,2-dichloroethane by *Xanthobacter autotrophicus*. *Appl. Environ. Microbiol.* **2000**, *66*, 4870–4876.
- (18) Rayleigh, J. W. S. Theoretical considerations respecting the separation of gases by diffusion and similar processes. *Philos. Mag.* **1896**, *42*, 493–498.
- (19) Mariotti, A.; Germon, J. C.; Hubert, P.; Kaiser, P.; Letolle, R.; Tardieux, A.; Tardieux, P. Experimental determination of nitrogen kinetic isotope fractionation: Some principles; illustration for the denitrification and nitrification processes. *Plant Soil* **1981**, *62*, 413–430.
- (20) Yoshida, N. N-15-depleted  $\text{N}_2\text{O}$  as a product of nitrification. *Nature* **1988**, *335*, 528–529.
- (21) Bigeleisen, J.; Wolfsberg, M. Theoretical and experimental aspects of isotope effects in chemical kinetics. *Adv. Chem. Phys.* **1958**, *1*, 15–76.
- (22) Melander, L.; Saunders, W. H. *Reaction rates of isotopic molecules*; John Wiley: New York, 1980; p 331.
- (23) Cook, P. F.; *Enzyme mechanism from isotope effects*; CRC Press: Boca Raton, 1991.
- (24) Meckenstock, R. U.; Morasch, B.; Griebler, C.; Richnow, H. H. Stable isotope fractionation analysis as a tool to monitor biodegradation in contaminated aquifers. *J. Contam. Hydrol.* **2004**, *75*, 215–255.
- (25) Eyring, H.; Cagle, F. W. The significance of isotopic reactions in rate theory. *J. Phys. Chem.* **1952**, *56*, 889–892.
- (26) Galimov, E. M. *The biological fractionation of isotopes*; Academic Press: Orlando, 1985.
- (27) Jancso, G.; Rebelo, L. P. N.; Vanhook, W. A. Isotope effects in solution thermodynamics – excess properties in solutions of isotopomers. *Chem. Rev.* **1993**, *93*, 2645–2666.
- (28) Szydłowski, J. Isotope effects on phase-equilibria in hydrogen-bonded systems, especially vapor-pressure and miscibility isotope effects. *J. Mol. Struct.* **1994**, *321*, 101–113.
- (29) Harrington, R. R.; Poulson, S. R.; Drever, J. I.; Colberg, P. J. S.; Kelly, E. F. Carbon isotope systematics of monoaromatic hydrocarbons: Vaporization and adsorption experiments. *Org. Geochem.* **1999**, *30*, 765–775.
- (30) Huang, L.; Sturchio, N. C.; Abrajano, T., Jr.; Heraty, L. J.; Holt, B. D. Carbon and chlorine isotope fractionation of chlorinated aliphatic hydrocarbons by evaporation. *Org. Geochem.* **1999**, *30*, 777–785.
- (31) Zhang, B. L.; Joutiteau, C.; Pionnier, S.; Gentil, E. Determination of multiple equilibrium isotopic fractionation factors at natural abundance in liquid–vapor transitions of organic molecules. *J. Phys. Chem. B* **2002**, *106*, 2983–2988.
- (32) Slater, G. F.; Ahad, J. M. E.; Sherwood Lollar, B.; Allen-King, R.; Sleep, B. Carbon isotope effects resulting from equilibrium sorption of dissolved VOCs. *Anal. Chem.* **2000**, *72*, 5669–5672.
- (33) Wade, D. Deuterium isotope effects on noncovalent interactions between molecules. *Chem. Biol. Interact.* **1999**, *117*, 191–217.
- (34) Rakowski, K.; Paneth, P. Isotope effects on binding. *J. Mol. Struct.* **1996**, *378*, 35–43.
- (35) Huskey, W. P. In *Enzyme mechanism from isotope effects*; Cook, P. F., Ed.; CRC Press: Boca Raton, FL, 1991; pp 37–72.
- (36) Paneth, P.; O'Leary, M. H. Nitrogen and deuterium-isotope effects on quaternization of *N,N*-dimethyl-para-toluidine. *J. Am. Chem. Soc.* **1991**, *113*, 1691–1693.
- (37) Marlier, J. F. Multiple isotope effects on the acyl group transfer reactions of amides and esters. *Acc. Chem. Res.* **2001**, *34*, 283–290.
- (38) Paneth, P. In *Isotopes in organic chemistry, Vol. 8: Heavy atom isotope effects*; Buncl, E., Saunders, W. H., Eds.; Elsevier: Amsterdam, London, New York, Tokyo, 1992; pp 41–68.
- (39) O'Leary, M. H. In *Enzyme kinetics and mechanism, part B: Isotopic probes and complex enzyme systems*; Purich, D. L., Ed.; Academic Press: New York, London, Toronto, Sydney, San Francisco, 1980; Vol. 64, pp 83–104.
- (40) Singleton, D. A.; Thomas, A. A. High-precision simultaneous determination of multiple small kinetic isotope effects at natural-abundance. *J. Am. Chem. Soc.* **1995**, *117*, 9357–9358.
- (41) Zhang, B. L.; Pionnier, S. A simple method for the precise and simultaneous determination of primary and multiple secondary kinetic deuterium isotope effects in organic reactions at natural abundance. *J. Phys. Org. Chem.* **2001**, *14*, 239–246.
- (42) Sühnel, J.; Schowen, R. L. In *Enzyme mechanism from isotope effects*; Cook, P. F., Ed.; CRC Press: Boca Raton, Ann Arbor, Boston, London, 1991; pp 3–35.
- (43) Thornton, E. R. A simple theory for predicting effects of substituent changes on transition-state geometry. *J. Am. Chem. Soc.* **1967**, *89*, 2915–&.
- (44) Westheimer, F. H. The magnitude of the primary kinetic isotope effect for compounds of hydrogen and deuterium. *Chem. Rev.* **1961**, *61*, 265–273.
- (45) Kirsch, J. F. In *Isotope effects on enzyme-catalyzed reactions*; Cleland, W. W., O'Leary, M. H., Northrop, D. B., Eds.; University Park Press: Baltimore, London, Tokyo, 1977; pp 100–121.
- (46) Westaway, K. C. In *Isotopes in organic chemistry, vol. 8: Secondary and solvent isotope effects*; Buncl, E., Lee, C. C., Eds.; Elsevier: Amsterdam, Oxford, New York, Tokyo, 1987; pp 275–392.
- (47) Merrigan, S. R.; Le Gloahec, V. N.; Smith, J. A.; Barton, D. H. R.; Singleton, D. A. Separation of the primary and secondary kinetic isotope effects at a reactive center using starting material reactivities. Application to the  $\text{FeCl}_3$ -catalyzed oxidation of C–H bonds with *tert*-butyl hydroperoxide. *Tetrahedron Lett.* **1999**, *40*, 3847–3850.
- (48) Roberts, A. L.; Gschwend, P. M. Interaction of abiotic and microbial processes in hexachloroethane reduction in groundwater. *J. Contam. Hydrol.* **1994**, *16*, 157–174.
- (49) Arnold, W. A.; Winget, P.; Cramer, C. J. Reductive dechlorination of 1,1,2,2-tetrachloroethane. *Environ. Sci. Technol.* **2002**, *36*, 3536–3541.
- (50) Singleton, D. A.; Merrigan, S. R.; Liu, J.; Houk, K. N. Experimental geometry of the epoxidation transition state. *J. Am. Chem. Soc.* **1997**, *119*, 3385–3386.
- (51) Bell, R. P. The tunnel effect correction for parabolic potential barriers. *Trans. Faraday Soc.* **1959**, *55*, 1–4.
- (52) Kresge, A. J. In *Isotope effects on enzyme-catalyzed reactions*; Cleland, W. W., O'Leary, M. H., Northrop, D. B., Eds.; University Park Press: Baltimore, London, Tokyo, 1977; pp 37–63.
- (53) Stewart, R. In *Isotopes in organic chemistry, Vol. 2: Isotopes in hydrogen transfer processes*; Buncl, E., Lee, C. C., Eds.; Elsevier: Amsterdam, Oxford, New York, 1976; pp 271–310.
- (54) Manchester, J. I.; Dinnocenzo, J. P.; Higgins, L. A.; Jones, J. P. A new mechanistic probe for cytochrome P450: An application of isotope effect profiles. *J. Am. Chem. Soc.* **1997**, *119*, 5069–5070.
- (55) Knapp, M. J.; Klinman, J. P. Environmentally coupled hydrogen tunneling – linking catalysis to dynamics. *Eur. J. Biochem.* **2002**, *269*, 3113–3121.



- (56) Shiner, V. J.; Wilgis, F. P. In *Isotopes in organic chemistry, Vol. 8: Heavy atom isotope effects*; Buncl, E., Saunders, W. H., Eds.; Amsterdam, London, New York, Tokyo, 1992; pp 239–335.
- (57) DelMonte, A. J.; Haller, J.; Houk, K. N.; Sharpless, K. B.; Singleton, D. A.; Strassner, T.; Thomas, A. A. Experimental and theoretical kinetic isotope effects for asymmetric dihydroxylation. Evidence supporting a rate-limiting “(3+2)” cycloaddition. *J. Am. Chem. Soc.* **1997**, *119*, 9907–9908.
- (58) Houk, K. N.; Strassner, T. Establishing the (3+2) mechanism for the permanganate oxidation of alkenes by theory and kinetic isotope effects. *J. Org. Chem.* **1999**, *64*, 800–802.
- (59) Northrop, D. B. The expression of isotope effects on enzyme-catalyzed reactions. *Annu. Rev. Biochem.* **1981**, *50*, 103–131.
- (60) Northrop, D. B. On the meaning of  $K_m$  and  $V/K$  in enzyme kinetics. *J. Chem. Educ.* **1998**, *75*, 1153–1157.
- (61) Pause, L.; Robert, M.; Saveant, J. M. Reductive cleavage of carbon tetrachloride in a polar solvent. An example of a dissociative electron transfer with significant attractive interaction between the caged product fragments. *J. Am. Chem. Soc.* **2000**, *122*, 9829–9835.
- (62) Elsner, M.; Haderlein, S. B.; Kellerhals, T.; Luzi, S.; Zwank, L.; Angst, W.; Schwarzenbach, R. P. Mechanisms and products of surface-mediated reductive dehalogenation of carbon tetrachloride by Fe(II) on goethite. *Environ. Sci. Technol.* **2004**, *38*, 2058–2066.
- (63) Scott, K. M.; Lu, X.; Cavanaugh, C. M.; Liu, J. S. Optimal methods for estimating kinetic isotope effects from different forms of the Rayleigh distillation equation. *Geochim. Cosmochim. Acta* **2004**, *68*, 433–442.
- (64) Hunkeler, D.; Butler, B. J.; Aravena, R.; Barker, J. F. Monitoring biodegradation of methyl *tert*-butyl ether (MTBE) using compound-specific carbon isotope analysis. *Environ. Sci. Technol.* **2001**, *35*, 676–681.
- (65) Gray, J. R.; Lacrampe-Couloume, G.; Gandhi, D.; Scow, K. M.; Wilson, R. D.; Mackay, D. M.; Sherwood Lollar, B. Carbon and hydrogen isotopic fractionation during biodegradation of methyl *tert*-butyl ether. *Environ. Sci. Technol.* **2002**, *36*, 1931–1938.
- (66) Morasch, B.; Richnow, H. H.; Vieth, A.; Schink, B.; Meckenstock, R. U. Stable isotope fractionation caused by glycol radical enzymes during bacterial degradation of aromatic compounds. *Appl. Environ. Microbiol.* **2004**, *70*, 2935–2940.
- (67) Rudolph, J.; Czuba, E.; Huang, L. The stable carbon isotope fractionation for reactions of selected hydrocarbons with OH-radicals and its relevance for atmospheric chemistry. *J. Geophys. Res., [Atmos.]* **2000**, *105*, 29329–29346.
- (68) Iannone, R.; Anderson, R. S.; Vogel, A.; Rudolph, J.; Eby, P.; Whittaker, M. J. Laboratory studies of the hydrogen kinetic isotope effects (KIEs) of the reaction of non-methane hydrocarbons with the OH radical in the gas phase. *J. Atmos. Chem.* **2004**, *47*, 191–208.
- (69) Monson, K. D.; Hayes, J. M. Carbon isotopic fractionation in the biosynthesis of bacterial fatty-acids – ozonolysis of unsaturated fatty-acids as a means of determining the intramolecular distribution of carbon isotopes. *Geochim. Cosmochim. Acta* **1982**, *46*, 139–149.
- (70) Rossmann, A.; Butzenlechner, M.; Schmidt, H. L. Evidence for a nonstatistical carbon isotope distribution in natural glucose. *Plant Physiol.* **1991**, *96*, 609–614.
- (71) Zwank, L.; Berg, M.; Elsner, M.; Schmidt, T. C.; Schwarzenbach, R. P.; Haderlein, S. B. A new evaluation scheme for two-dimensional isotope analysis to decipher biodegradation processes: Application to groundwater contamination by MTBE. *Environ. Sci. Technol.* **2005**, *39*, 1018–1029.
- (72) Martin, G. J. Recent advances in site-specific natural isotope fractionation studied by nuclear magnetic resonance. *Isotopes Environ. Health Stud.* **1998**, *34*, 233–243.
- (73) Mancini, S. A.; Ulrich, A. E.; Lacrampe-Couloume, G.; Sleep, B.; Edwards, E. A.; Sherwood Lollar, B. Carbon and hydrogen isotopic fractionation during anaerobic biodegradation of benzene. *Appl. Environ. Microbiol.* **2003**, *69*, 191–198.
- (74) Griebler, C.; Adrian, L.; Meckenstock, R. U.; Richnow, H. H. Stable carbon isotope fractionation during aerobic and anaerobic transformation of trichlorobenzene. *FEMS Microbiol. Ecol.* **2004**, *48*, 313–321.
- (75) Ahad, J. M. E.; Sherwood Lollar, B.; Edwards, E. A.; Slater, G. F.; Sleep, B. E. Carbon isotope fractionation during anaerobic biodegradation of toluene: Implications for intrinsic bioremediation. *Environ. Sci. Technol.* **2000**, *34*, 892–896.
- (76) Morasch, B.; Richnow, H. H.; Schink, B.; Meckenstock, R. U. Stable hydrogen and carbon isotope fractionation during microbial toluene degradation: Mechanistic and environmental aspects. *Appl. Environ. Microbiol.* **2001**, *67*, 4842–4849.
- (77) Miller, L. G.; Kalin, R. M.; McCauley, S. E.; Hamilton, J. T. G.; Harper, D. B.; Millet, D. B.; Oremland, R. S.; Goldstein, A. H. Large carbon isotope fractionation associated with oxidation of methyl halides by methylotrophic bacteria. *Proc. Natl. Acad. Sci. U.S.A.* **2001**, *98*, 5833–5837.
- (78) Coleman, N. V.; Spain, J. C. Epoxyalkane: Coenzyme M transferase in the ethene and vinyl chloride biodegradation pathways of *Mycobacterium* strain JS60. *J. Bacteriol.* **2003**, *185*, 5536–5545.
- (79) Chu, K. H.; Mahendra, S.; Song, D. L.; Conrad, M. E.; Alvarez-Cohen, L. Stable carbon isotope fractionation during aerobic biodegradation of chlorinated ethenes. *Environ. Sci. Technol.* **2004**, *38*, 3126–3130.
- (80) Barth, J. A. C.; Slater, G.; Schueth, C.; Bill, M.; Downey, A.; Larkin, M.; Kalin, R. M. Carbon isotope fractionation during aerobic biodegradation of trichloroethene by *Burkholderia cepacia* G4: A tool to map degradation mechanisms. *Appl. Environ. Microbiol.* **2002**, *68*, 1728–1734.
- (81) Zwank, L.; Elsner, M.; Aeberhard, A.; Schwarzenbach, R. P.; Haderlein, S. B. Carbon isotope fractionation in the reductive dehalogenation of carbon tetrachloride at iron (hydr)oxide and iron sulfide minerals. *Environ. Sci. Technol.* **2005**, *31*, 5634–5641.
- (82) Glod, G.; Angst, W.; Holliger, C.; Schwarzenbach, R. P. Corrinoid-mediated reduction of tetrachloroethylene, trichloroethylene and trichlorofluoroethane in homogeneous aqueous solution: Reaction kinetics and reaction mechanisms. *Environ. Sci. Technol.* **1997**, *31*, 253–260.
- (83) Glod, G.; Brodmann, U.; Werner, A.; Holliger, C.; Schwarzenbach, R. P. Cobalamin-mediated reduction of *cis*- and *trans*-dichloroethene, and vinyl chloride in homogeneous aqueous solution: Reaction kinetics and mechanistic considerations. *Environ. Sci. Technol.* **1997**, *31*, 3154–3160.
- (84) Shey, J.; van der Donk, W. A. Mechanistic studies on the vitamin B12-catalyzed dechlorination of chlorinated alkenes. *J. Am. Chem. Soc.* **2000**, *122*, 12403–12404.
- (85) Slater, G. F.; Sherwood Lollar, B.; Lesage, S.; Brown, S. Carbon isotope fractionation of PCE and TCE during dechlorination by vitamin B12. *Groundwater Monit. Remed.* **2003**, *23*, 59–67.
- (86) Bloom, Y.; Aravena, R.; Hunkeler, D.; Edwards, E.; Frappe, S. K. Carbon isotope fractionation during microbial dechlorination of trichloroethene, *cis*-1,2-dichloroethene, and vinyl chloride: Implications for assessment of natural attenuation. *Environ. Sci. Technol.* **2000**, *34*, 2768–2772.
- (87) Slater, G. F.; Sherwood Lollar, B.; Sleep, B. E.; Edwards, E. A. Variability in carbon isotopic fractionation during biodegradation of chlorinated ethenes: Implications for field applications. *Environ. Sci. Technol.* **2001**, *35*, 901–907.
- (88) Hunkeler, D.; Aravena, R.; Cox, E. Carbon isotopes as a tool to evaluate the origin and fate of vinyl chloride: Laboratory experiments and modeling of isotope evolution. *Environ. Sci. Technol.* **2002**, *36*, 3378–3384.
- (89) Arnold, W. A.; Roberts, A. L. Pathways and kinetics of chlorinated ethylene and chlorinated acetylene reaction with Fe(0) particles. *Environ. Sci. Technol.* **2000**, *34*, 1794–1805.
- (90) VanStone, N. A.; Focht, R. M.; Mabury, S. A.; Sherwood Lollar, B. Effect of iron type on kinetics and carbon isotopic enrichment of chlorinated ethylenes during abiotic reduction on Fe(0). *Ground Water* **2004**, *42*, 268–276.
- (91) Dayan, H.; Abrajano, T.; Sturchio, N. C.; Winsor, L. Carbon isotopic fractionation during reductive dehalogenation of chlorinated ethenes by metallic iron. *Org. Geochem.* **1999**, *30*, 755–763.
- (92) Slater, G.; Sherwood Lollar, B.; Allen King, R.; O'Hannesin, S. F. Isotopic fractionation during reductive dechlorination of trichloroethene by zerovalent iron: Influence of surface treatment. *Chemosphere* **2002**, *49*, 587–596.
- (93) Bill, M.; Schueth, C.; Barth, J. A. C.; Kalin, R. M. Carbon isotope fractionation during abiotic reductive dehalogenation of trichloroethene (TCE). *Chemosphere* **2001**, *44*, 1281–1286.
- (94) Kuder, T.; Wilson, J. T.; Kaiser, P.; Kolhatkar, R.; Philp, P.; Allen, J. Enrichment of stable carbon and hydrogen isotopes during anaerobic biodegradation of MTBE: Microcosm and field evidence. *Environ. Sci. Technol.* **2005**, *39*, 213–220.
- (95) Hirschorn, S. K.; Dinglasan, M. J.; Elsner, M.; Mancini, S. A.; Lacrampe-Couloume, G.; Edwards, E. A.; Sherwood Lollar, B. Pathway dependent isotopic fractionation during aerobic biodegradation of 1,2-dichloroethane. *Environ. Sci. Technol.* **2004**, *38*, 4775–4781.



- (96) Hunkeler, D.; Andersen, N.; Aravena, R.; Bernasconi, S. M.; Butler, B. J. Hydrogen and carbon isotope fractionation during aerobic biodegradation of benzene. *Environ. Sci. Technol.* **2001**, *35*, 3462–3467.
- (97) Sherwood Lollar, B.; Slater, G. F.; Sleep, B.; Witt, M.; Klecka, G. M.; Harkness, M.; Spivack, J. Stable carbon isotope evidence for intrinsic bioremediation of tetrachloroethene and trichloroethene at area 6, Dover air force base. *Environ. Sci. Technol.* **2001**, *35*, 261–269.
- (98) Mancini, S. A.; Lacrampe-Couloume, G.; Jonker, H.; Van Breukelen, B. M.; Groen, J.; Volkering, F.; Sherwood Lollar, B. Hydrogen isotopic enrichment: An indicator of biodegradation at a petroleum hydrocarbon contaminated field site. *Environ. Sci. Technol.* **2002**, *36*, 2464–2470.
- (99) Griebler, C.; Safinowski, M.; Vieth, A.; Richnow, H. H.; Meckenstock, R. U. Combined application of stable carbon isotope analysis and specific metabolites determination for assessing in situ degradation of aromatic hydrocarbons in a tar oil-contaminated aquifer. *Environ. Sci. Technol.* **2004**, *38*, 617–631.
- (100) Peter, A.; Steinbach, A.; Liedl, R.; Ptak, T.; Michaelis, W.; Teutsch, G. Assessing microbial degradation of *o*-xylene at field-scale from the reduction in mass flow rate combined with compound-specific isotope analyses. *J. Contam. Hydrol.* **2004**, *71*, 127–154.
- (101) Richnow, H. H.; Meckenstock, R. U.; Reitzel, L. A.; Baun, A.; Ledin, A.; Christensen, T. H. In situ biodegradation determined by carbon isotope fractionation of aromatic hydrocarbons in an anaerobic landfill leachate plume (Vejen, Denmark). *J. Contam. Hydrol.* **2003**, *64*, 59–72.
- (102) Richnow, H. H.; Annweiler, E.; Michaelis, W.; Meckenstock, R. U. Microbial in situ degradation of aromatic hydrocarbons in a contaminated aquifer monitored by carbon isotope fractionation. *J. Contam. Hydrol.* **2003**, *65*, 101–120.
- (103) Morrill, P. L.; Lacrampe-Couloume, G.; Slater, G. F.; Sleep, B. E.; Edwards, E. A.; McMaster, M. L.; Major, D. W.; Lollar, B. S. Quantifying chlorinated ethene degradation during reductive dechlorination at Kelly AFB using stable carbon isotopes. *J. Contam. Hydrol.* **2005**, *76*, 279–293.
- (104) Steinbach, A.; Seifert, R.; Annweiler, E.; Michaelis, W. Hydrogen and carbon isotope fractionation during anaerobic biodegradation of aromatic hydrocarbons – a field study. *Environ. Sci. Technol.* **2004**, *38*, 609–616.
- (105) Kolhatkar, R.; Kuder, T.; Philip, P.; Allen, J.; Wilson, J. T. Use of compound-specific stable carbon isotope analyses to demonstrate anaerobic biodegradation of MTBE in groundwater at a gasoline release site. *Environ. Sci. Technol.* **2002**, *36*, 5139–5146.
- (106) Lewandowicz, A.; Rudzinski, J.; Tronstad, L.; Widersten, M.; Ryberg, P.; Matsson, O.; Paneth, P. Chlorine kinetic isotope effects on the haloalkane dehalogenase reaction. *J. Am. Chem. Soc.* **2001**, *123*, 4550–4555.
- (107) Willi, A. V. *Isotopeneffekte bei chemischen Reaktionen*; Georg Thieme Verlag: Stuttgart, New York, 1983.
- (108) Anderson, V. E. In *Enzyme mechanism from isotope effects*; Cook, P. F., Ed.; CRC Press: Boca Raton, FL, 1991; pp 389–418.
- (109) Koch, H. F.; Lodder, G.; Koch, J. G.; Bogdan, D. J.; Brown, G. H.; Carlson, C. A.; Dean, A. B.; Hage, R.; Han, P.; Hopman, J. C. P.; James, L. A.; Knape, P. M.; Roos, E. C.; Sardina, M. L.; Sawyer, R. A.; Scott, B. O.; Testa, C. A.; Wickham, S. D. Use of kinetic isotope effects in mechanism studies. Isotope effects and element effects associated with hydrogen-transfer steps during alkoxide-promoted dehydrohalogenations. *J. Am. Chem. Soc.* **1997**, *119*, 9965–9974.
- (110) Cleland, W. W.; Hengge, A. C. Mechanisms of phosphoryl and acyl transfer. *FASEB J.* **1995**, *9*, 1585–1594.
- (111) Hengge, A. C.; Cleland, W. W. Phosphoryl-transfer reactions of phosphodiesterases – characterization of transition-states by heavy-atom isotope effects. *J. Am. Chem. Soc.* **1991**, *113*, 5835–5841.
- (112) Hengge, A. C.; Edens, W. A.; Elsing, H. Transition-state structures for phosphoryl-transfer reactions of *p*-nitrophenyl phosphate. *J. Am. Chem. Soc.* **1994**, *116*, 5045–5049.
- (113) Grzyska, P. K.; Czyryca, P. G.; Purcell, J.; Hengge, A. C. Transition state differences in hydrolysis reactions of alkyl versus aryl phosphate monoester monoanions. *J. Am. Chem. Soc.* **2003**, *125*, 13106–13111.
- (114) Hengge, A. C.; Sowa, G. A.; Wu, L.; Zhang, Z. Y. Nature of the transition-state of the protein-tyrosine phosphatase-catalyzed reaction. *Biochemistry* **1995**, *34*, 13982–13987.
- (115) Catrina, I. E.; Hengge, A. C. Comparisons of phosphorothioate with phosphate transfer reactions for a monoester, diester, and triester: Isotope effect studies. *J. Am. Chem. Soc.* **2003**, *125*, 7546–7552.
- (116) Hengge, A. C. Isotope effects in the study of phosphoryl and sulfuryl transfer reactions. *Acc. Chem. Res.* **2002**, *35*, 105–112.
- (117) Gilliom, R. D.; Brewer, R. M.; Miller, K. R. Temperature-dependence of the kinetic isotope effect in the homolytic abstraction of benzylic hydrogen by bromine. *J. Org. Chem.* **1983**, *48*, 3600–3601.
- (118) Rudakov, E. S.; Tishchenko, N. A. Temperature rate dependence, kinetic hydrogen isotope effect, and 5/6 effect for the reactions of cyclopentane and cyclohexane with oxidants and electrophiles. 6. Kinetic isotope effect and reagent structure. *Kinet. Catal.* **1990**, *31*, 945–951.
- (119) Amin, M.; Saunders, W. H. Temperature-dependence of the deuterium-isotope effect in the deprotonation of some nitroalkanes by anionic bases. *J. Phys. Org. Chem.* **1993**, *6*, 393–398.
- (120) Zielinski, M.; Zielinska, A.; Papiernik, Zielinska, H. Temperature dependence of the carbon-13 isotope effect in the decarboxylation of concentrated formic acid solutions of sodium chloride and of metaphosphoric acid reagent. *Isot. Environ. Health Stud.* **1996**, *32*, 31–39.
- (121) Zielinski, M.; Zielinska, A.; Paul, H.; Bernasconi, S.; Ogrinc, N.; Kobal, I.; Papiernik-Zielinska, H. Carbon-13 isotope effect in the decarboxylation of phenylpropionic acid in sulphuric acid. *Pol. J. Chem.* **1999**, *73*, 1029–1036.
- (122) Bigeleisen, J.; Yankwich, P. E.; Haschemeyer, R. H.; Wolfsberg, M. Temperature dependence of carbon isotope effect in dehydration of formic acid by concentrated sulfuric acid. *J. Am. Chem. Soc.* **1962**, *84*, 1813–&.
- (123) Yankwich, P. E.; Veazie, A. E. Temperature dependence of the carbon isotope effect in the acid hydrolysis of urea. *J. Am. Chem. Soc.* **1958**, *80*, 1835–1838.
- (124) Leskovac, V.; Trivic, S.; NikolicDjoric, E. Temperature dependence of the primary kinetic isotope effect in hydride transfer reactions with NAD(+) and NADH models. *Bioorg. Chem.* **1997**, *25*, 1–10.
- (125) Siebrand, W.; Smedarchina, Z. Temperature dependence of kinetic isotope effects for enzymatic carbon–hydrogen bond cleavage. *J. Phys. Chem. B* **2004**, *108*, 4185–4195.
- (126) Ward, J. A. M.; Ahad, J. M. E.; Lacrampe-Couloume, G.; Slater, G. F.; Edwards, E. A.; Sherwood Lollar, B. Hydrogen isotope fractionation during methanogenic degradation of toluene: Potential for direct verification of bioremediation. *Environ. Sci. Technol.* **2000**, *34*, 4577–4581.
- (127) Hunkeler, D.; Meckenstock, R. U.; Richnow, H. H. Quantification of isotope fractionation in experiments with deuterium-labeled substrate; letter to the editor and reply. *Appl. Environ. Microbiol.* **2002**, *68*, 5205–5207.
- (128) Kalin, R. M.; Hamilton, J. T. G.; Harper, D. B.; Miller, L. G.; Lamb, C.; Kennedy, J. T.; Downey, A.; McCauley, S.; Goldstein, A. H. Continuous flow stable isotope methods for study of delta C-13 fractionation during halomethane production and degradation. *Rapid Commun. Mass Spectrom.* **2001**, *15*, 357–363.
- (129) Miller, L. G.; Warner, K. L.; Baesman, S. M.; Oremland, R. S.; McDonald, I. R.; Radajewski, S.; Murrell, J. C. Degradation of methyl bromide and methyl chloride in soil microcosms: Use of stable C isotope fractionation and stable isotope probing to identify reactions and the responsible microorganisms. *Geochim. Cosmochim. Acta* **2004**, *68*, 3271–3283.
- (130) Poulson, S. R.; Naraoka, H. Carbon isotope fractionation during permanganate oxidation of chlorinated ethylenes (cDCE, TCE, PCE). *Environ. Sci. Technol.* **2002**, *36*, 3270–3274.
- (131) Chartrand, M. G.; Waller, A.; Mattes, T. E.; Elsner, M.; Lacrampe-Couloume, G.; Gossett, J. M.; Edwards, E. A.; Sherwood Lollar, B. Carbon isotopic fractionation during aerobic vinyl chloride biodegradation. *Environ. Sci. Technol.* **2005**, *39*, 1064–1070.
- (132) Somsamak, P.; Richnow, H. H.; Haggblom, M. M. Carbon isotopic fractionation during anaerobic biotransformation of methyl *tert*-butyl ether and *tert*-amyl methyl ether. *Environ. Sci. Technol.* **2005**, *39*, 103–109.
- (133) Hunkeler, D.; Aravena, R.; Cherry, J. A.; Parker, B. Carbon isotope fractionation during chemical oxidation of chlorinated ethenes by permanganate: Laboratory and field studies. *Environ. Sci. Technol.* **2003**, *37*, 798–804.